5

RADIATIVE TRANSFER THEORY FOR ACTIVE REMOTE SENSING OF TWO-LAYER RANDOM MEDIUM

R. T. Shin and J. A. Kong

5.1 Introduction

The remote sensing of the earth and the elements of its environment at microwave frequencies have been found to contain many practical applications. The primary advantage inherent in remote sensing at microwave frequencies over optical and infrared frequencies is in its all-weather, day-and-night operational capabilities. Active and passive microwave remote sensing with both radar and radiometer have been investigated in areas of snow and ice covered land or water [1–15], veg-

etation canopy [16–19], cloud and rainfall [20,21], and soil moisture studies [22–30]. While extensive effort has been concentrated in the measurement and collection of voluminous experimental data, theoretical models that are useful in interpreting these data have not been satisfactorily developed, especially where combinations of absorption, scattering, layering and rough surface are important factors. Although past theoretical emphasis has been largely concentrated on rough surface scattering, recent theoretical models have been proposed to account for volume scattering effects [31].

In the active and passive microwave remote sensing of earth terrain, the scattering effects due to medium inhomogeneities and rough interfaces play a dominant role in the determination of brightness temperatures and radar backscattering coefficients. The effects of volume scattering have been treated with two theoretical models for the terrain media: (1) the random medium model where scattering effects can be accounted for by introducing a randomly fluctuating part in the permittivities, and (2) the discrete scatterer model where discrete scatterers are imbedded in a homogeneous background medium.

In the theoretical developments for passive remote sensing the effect of volume scattering due to medium inhomogeneity was first accounted for by Gurvich et al., [32]. They derived expressions for the brightness temperature of a halfspace random medium with a laminar structure, assuming uniform temperature distribution. Tsang and Kong [33] solved the problem of thermal microwave emission from a halfspace random medium with a laminar structure and nonuniform temperature distribution using the radiative transfer theory. England [34] first examined thermal microwave emission from a uniform low-loss dielectric medium containing randomly distributed isotropic scatterers, with a radiative transfer approach. He [35] then considered the more general case of a scattering layer over a homogeneous halfspace, using the radiative transfer theory and a Rayleigh scattering model. Tsang and Kong [36] derived a more general result than that of England for both the halfspace and two-layer case, using a Mie scattering model. With the Born approximation, Tsang and Kong [37] obtained the emissivity of a halfspace random medium with a three-dimensional variation.

In active remote sensing, Stogryn [38] first calculated the bistatic scattering coefficients for a random medium with a spherical correlation function using a perturbation approach. Leader [39] studied scat-

tering from Rayleigh scatterers imbedded in a dielectric slab using the matrix doubling method. Using the Born approximation, Tsang and Kong [36] studied scattering of electromagnetic waves by a halfspace random medium. They [40] also developed the radiative transfer theory to calculate the bistatic scattering coefficients from a halfspace random medium. An iterative approach is used to obtain results to the second order, in order to exhibit depolarizaton of backscattered power. Using the first-order renormalization method, Fung and Fung [41] obtained the bistatic scattering coefficients from a vegetation-like halfspace random medium. Fung [42] then extended the result to the case of a vegetation-like layer over a homogeneous halfspace. Zuniga and Kong [43] studied the scattering from a slab of random medium using the Born approximation. Then, Zuniga et al., [44] extended the result to the second order in albedo to show the depolarization effect in the backscattering direction.

The radiative transfer theory has been useful in the interpretation of remote sensing data [45]. Even though it deals only with the intensities of the field quantities and neglects their coherent nature, it accounts for the multiple scattering and obeys energy conservation. The modified radiative transfer (MRT) theory [46–48] which takes into account the partial coherent effects due to the boundaries has been derived for the cases when the interference effects become important [49]. The MRT equations have been developed for a two-layer random medium with laminar structure by applying the nonlinear approximation to Dyson's equation and the ladder approximation to the Bethe-Salpeter equation [46]. Then, the MRT equations for electromagnetic wave propogation in a two-layer medium with three-dimensional permittivity fluctuations are derived [47,48]. The MRT equations are then solved with the first order renormalization approximation to obtain the backscattering cross sections.

Most of the previous work on volume scattering all assumed planar boundaries, and the effect of rough surface scattering was neglected. However, in order to understand in a more meaningful way the problems of radar backscattering and thermal microwave emission from natural terrains, a composite model that can account for both the volume and surface scattering effects must be studied. Recently, the Rayleigh scattering model has been used with the radiative transfer equations to study the combined volume and rough surface scattering effects [50–52].

In this chapter, we solve the problem of scattering from a two-layer random medium using the radiative transfer theory. The volume scattering effect is first studied in section 5.2 by considering the two-layer random medium with planar interfaces. Using all four Stokes parameters, the bistatic scattering coefficients of two-layer random medium are first calculated using a numerical approach which provides a valid solution for both small and large albedos. A Fourier-series expansion in the azimuthal direction is used to eliminate the azimuthal ϕ-dependence from the radiative transfer equations. Then, the set of equations without the ϕ-dependence is solved using the method of Gaussian quadrature. The integrals in the radiative transfer equations are replaced by a Gaussian quadrature and the resulting system of first-order differential equations is solved by obtaining eigenvalues and eigenvectors and matching the boundary conditions. The order of the system of eigen-equations is reduced for more efficient computation by making use of the symmetry properties of the scattering function matrix. The numerical results are illustrated by plotting backscattering cross sections and the bistatic scattering coefficients as functions of frequency, incident angle, and the scattering angles.

In section 5.3, the combined volume and rough surface scattering effects are studied with a two-layer random medium model with rough interfaces. The rough surface effects are incorporated into the radiative transfer equations by modifying the boundary conditions. The reflected and transmitted bistatic scattering coefficients derived with the randomly rough surface models are used to derived the boundary conditions satisfied by the intensities at the top and bottom interfaces. The radiative transfer equations are again solved numerically using the Fourier-series expansion and the Gaussian quadrature method. The thoeretical results are illustrated by plotting the backscattering cross sections as functions of frequency and incident angle.

5.2   Two-Layer Random Medium with Planar Interfaces

a. Formulation

Consider a layer of random medium characterized by the permittivity $\epsilon_1 + \epsilon_f$, where ϵ_f stands for the randomly fluctuating part whose amplitude is very small and whose ensemble average is zero, on top of a

incident intensity z scattered intensity

Region 0 ϵ_0

θ_{oi} θ_{os}

$z = 0$

θ_s

Region 1 $\epsilon_1 = \epsilon_{1m} + \epsilon_{1f}(\bar{r}), \delta, l_z, l_p$

$< \epsilon_{1f}(\bar{r})\epsilon_{1f}^*(\bar{r}') >= \epsilon_{1m}^{\prime 2}\delta \exp[-\frac{(x-x')^2+(y-y')^2}{l_p^2} - \frac{|z-z'|}{l_z}]$
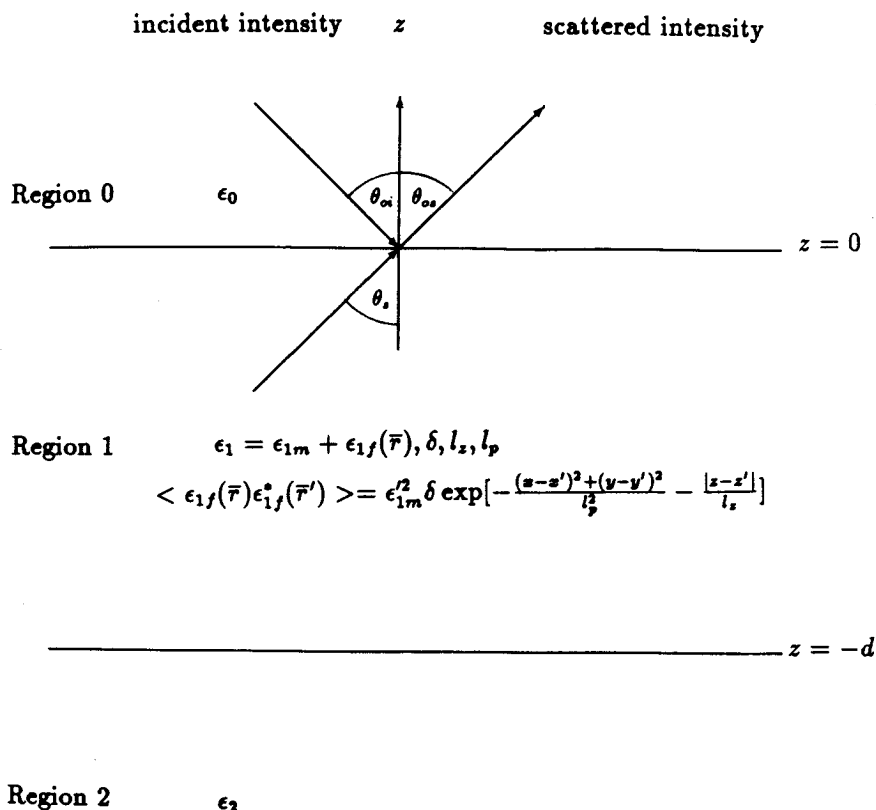
$z = -d$

Region 2 ϵ_2

Figure 5.2.1 Geometrical configuration of the problem.

homogeneous medium with permittivity ϵ_2 [Fig. 5.2.1]. The radiative transfer equations which govern the propagation of intensities inside the scattering medium are, for $0 < \theta < \pi$,

$$\cos\theta \frac{d}{dz}\bar{I}(\theta, \phi, z) = -K_a\bar{I}(\theta, \phi, z) - \overline{\overline{K}}_s(\theta) \cdot \bar{I}(\theta, \phi, z)$$

$$+ \int_0^\pi d\theta' \sin\theta' \int_0^{2\pi} d\phi' \overline{\overline{P}}(\theta, \phi; \theta'\phi') \cdot \bar{I}(\theta', \phi', z) \quad (1)$$

where

$$\bar{I}(\theta, \phi, z) = \begin{bmatrix} I_v(\theta, \phi, z) \\ I_h(\theta, \phi, z) \\ U(\theta, \phi, z) \\ V(\theta, \phi, z) \end{bmatrix} \tag{2}$$

I_v is the vertically polarized specific intensity, I_h is the horizontally polarized specific intensity, and U and V represent the correlation between two polarizations [40,53], $\overline{\overline{P}}(\theta, \phi; \theta', \phi')$ is a 4×4 scattering function matrix, which relates scattered intensities into the direction (θ, ϕ) from the incident intensities in the direction (θ', ϕ'), K_a is the loss per unit length due to absorption, and $\overline{\overline{K}}_s(\theta)$ is the loss per unit length due to scattering. The random permittivity fluctuation is characterized by the variance of the fluctuation δ and the correlation function with lateral correlation length l_ρ and vertical correlation length l_z. The scattering function matrix and the scattering coefficient have been derived by applying Born approximation with the far-field solution and the explicit expressions for the correlation function with gaussian dependence laterally and exponential dependence vertically are given in Appendix A [40].

Consider an incident wave with specific intensity $\bar{I}_{oi}(\pi - \theta_o, \phi_o)$ impinging from region 0, which is assumed to be free space, upon the scattering layer. The incident beam in region 0 assumes the form

$$\bar{I}_{oi}(\pi - \theta_o, \phi_o) = \bar{I}_{oi} \, \delta(\cos \theta_o - \cos \theta_{oi}) \, \delta(\phi_o - \phi_{oi}) \tag{3}$$

where the use of Dirac delta function is made.

The boundary conditions for the four Stokes parameters at a planar dielectric interface have been derived [40] from the continuity of tangential electric and magnetic fields. The results are, for $0 < \theta < \pi/2$, at $z = 0$,

$$\bar{I}(\pi - \theta, \phi, z = 0) = \overline{\overline{T}}_{01}(\theta_o) \cdot \bar{I}_{oi}(\pi - \theta_o, \phi_o) + \overline{\overline{R}}_{10}(\theta) \cdot \bar{I}(\theta, \phi, z = 0) \tag{4}$$

and, at $z = -d$,

$$\bar{I}(\theta, \phi, z = -d) = \overline{\overline{R}}_{12}(\theta) \cdot \bar{I}(\pi - \theta, \phi, z = -d) \tag{5}$$

where we have broken up intensities in the scattering layer into upward going intensities $\bar{I}(\theta, \phi, z)$ and downward going intensities $\bar{I}(\pi -$

$\theta, \phi, z)$. In the above equations, $\overline{\overline{T}}_{01}(\theta_o)$ represents the coupling from region 0 to region 1, $\overline{\overline{R}}_{10}(\theta)$ represents the coupling from upward going intensities into downward going intensities at the boundary of region 1 and region 0, and $\overline{\overline{R}}_{12}(\theta)$ represents similar coupling at the boundary of region 1 and region 2 [Appendix B].

Once the radiative transfer equations are solved subject to the boundary conditions (4) and (5), the intensity in the direction (θ_{os}, ϕ_{os}) in region 0 is

$$\overline{I}_o(\theta_{os}, \phi_{os}) = \overline{\overline{T}}_{10}(\theta_s) \cdot \overline{I}(\theta_s, \phi_s, z = 0) + \overline{\overline{R}}_{01}(\theta_o) \cdot \overline{I}_{oi}(\pi - \theta_o, \phi_o) \quad (6)$$

where $\overline{\overline{T}}_{10}(\theta)$ represents the coupling from region 1 to region 0. The bistatic scattering coefficients $\gamma_{\beta\alpha}(\theta_{os}, \phi_{os}; \theta_{oi}, \phi_{oi})$ are defined as the ratio of the scattered power of polarization β per unit solid angle in the direction (θ_{os}, ϕ_{os}) and the intercepted incident power of polarization α in the direction (θ_{oi}, ϕ_{oi}) averaged over 4π radians [54].

$$\gamma_{\beta\alpha}(\theta_{os}, \phi_{os}; \theta_{oi}, \phi_{oi}) = 4\pi \frac{\cos\theta_{os} \, I_{o\beta s}(\theta_{os}, \phi_{os})}{\cos\theta_{oi} \, I_{o\alpha i}} \quad (7)$$

where $\alpha, \beta = v$ or h with v denoting vertical polarization and h denoting horizontal polarization. In the backscattering direction $\theta_{os} = \theta_{oi}$ and $\phi_{os} = \pi - \phi_{oi}$. The backscattering cross sections per unit area are defined to be

$$\sigma_{\beta\alpha}(\theta_{oi}) = \cos\theta_{oi} \, \gamma_{\beta\alpha}(\theta_{oi}, \pi + \phi_{oi}; \theta_{oi}, \phi_{oi}) \quad (8)$$

b. Fourier Series Expansion

The radiative transfer equations can be solved using an iterative approach which gives closed form solutions [40,53] when the effect of scattering is small (small albedo). The radiative transfer equations and the boundary conditions are cast into the integral equation form, then an iterative process is applied to solve the integral equation to both the first and second order in albedo. The depolarization of the backscattered intensities has been shown to be the second-order effect. However, for the general cases when the effect of scattering is not small, we must resort to the numerical approach to solve the radiative transfer equations. We first use a Fourier-series expansion in the azimuthal direction

to eliminate the ϕ-dependence from the radiative transfer equations. We let

$$\bar{I}(\theta, \phi, z) = \sum_{m=0}^{\infty} \left[\bar{I}^{mc}(\theta, z) \cos m(\phi - \phi_i) + \bar{I}^{ms}(\theta, z) \sin m(\phi - \phi_i) \right]$$

(9)

$$\bar{\bar{P}}(\theta, \phi; \theta'\phi') = \sum_{m=0}^{\infty} \frac{1}{(1 + \delta_m)\pi}$$
$$\times \left[\bar{\bar{P}}^{mc}(\theta, \theta') \cos m(\phi - \phi') + \bar{\bar{P}}^{ms}(\theta, \theta') \sin m(\phi - \phi') \right]$$

(10)

where superscript m indicates the order of harmonics in the azimuthal direction, superscripts c and s indicate the cosine and sine dependence, and Neumann number $\delta_m = 0$ for $m \neq 0$ and $\delta_o = 1$. Also note that the zeroth-order sine dependence terms are zero.

$$\bar{I}^{os}(\theta, z) = 0 \tag{11a}$$

$$\bar{\bar{P}}^{os}(\theta, \theta') = 0 \tag{11b}$$

Substituting (9) and (10) into the radiative transfer equations, the ϕ'-integration can be carried out. Then, by collecting terms with the same sine or cosine dependence, we obtain a set of equations without the ϕ dependence. For $m = 0, 1, 2, \cdots$

$$\cos\theta \frac{d}{dz}\bar{I}^{mc}(\theta, z) = - K_a \bar{I}^{mc}(\theta, z) - \bar{\bar{K}}_s(\theta) \cdot \bar{I}^{mc}(\theta, z) + \int_0^\pi d\theta' \sin\theta'$$
$$\times \left[\bar{\bar{P}}^{mc}(\theta, \theta') \cdot \bar{I}^{mc}(\theta', z) - \bar{\bar{P}}^{ms}(\theta, \theta') \cdot \bar{I}^{ms}(\theta', z) \right]$$

(12a)

$$\cos\theta \frac{d}{dz}\bar{I}^{ms}(\theta, z) = - K_a \bar{I}^{ms}(\theta, z) - \bar{\bar{K}}_s(\theta) \cdot \bar{I}^{ms}(\theta, z) + \int_0^\pi d\theta' \sin\theta'$$
$$\times \left[\bar{\bar{P}}^{ms}(\theta, \theta') \cdot \bar{I}^{mc}(\theta', z) + \bar{\bar{P}}^{mc}(\theta, \theta') \cdot \bar{I}^{ms}(\theta', z) \right]$$

(12b)

The closed form expressions for the Fourier-series expanded scattering function matrices $\overline{\overline{P}}^{mc}(\theta,\theta')$ and $\overline{\overline{P}}^{ms}(\theta,\theta')$ are obtained [Appendix C]. We note that for azimuthally isotropic media the scattering function matrix can be expanded as

$$\overline{\overline{P}}^{mc}(\theta,\theta') = \begin{bmatrix} P_{11}^{mc} & P_{12}^{mc} & 0 & 0 \\ P_{21}^{mc} & P_{22}^{mc} & 0 & 0 \\ 0 & 0 & P_{33}^{mc} & P_{34}^{mc} \\ 0 & 0 & P_{43}^{mc} & P_{44}^{mc} \end{bmatrix} \qquad (13a)$$

$$\overline{\overline{P}}^{ms}(\theta,\theta') = \begin{bmatrix} 0 & 0 & P_{13}^{ms} & P_{14}^{ms} \\ 0 & 0 & P_{23}^{ms} & P_{24}^{ms} \\ P_{31}^{ms} & P_{32}^{ms} & 0 & 0 \\ P_{41}^{ms} & P_{42}^{ms} & 0 & 0 \end{bmatrix} \qquad (13b)$$

Thus, the coupled equations (12a) and (12b) can be changed into two decoupled equations by defining

$$\overline{I}^{me}(\theta,z) = \begin{bmatrix} I_v^{mc}(\theta,z) \\ I_h^{mc}(\theta,z) \\ U^{ms}(\theta,z) \\ V^{ms}(\theta,z) \end{bmatrix} \qquad (14a)$$

$$\overline{I}^{mo}(\theta,z) = \begin{bmatrix} I_v^{ms}(\theta,z) \\ I_h^{ms}(\theta,z) \\ U^{mc}(\theta,z) \\ V^{mc}(\theta,z) \end{bmatrix} \qquad (14b)$$

where superscripts e and o stands for even or odd dependence in the first two Stokes parameters. Decoupled equations are given by, for $m = 0,1,2,\cdots$

$$\cos\theta\frac{d}{dz}\overline{I}^{me}(\theta,z) = -K_a\overline{I}^{me}(\theta,z) - \overline{\overline{K}}_s(\theta)\cdot\overline{I}^{me}(\theta,z)$$
$$+ \int_0^\pi d\theta'\sin\theta'\overline{\overline{P}}^{me}(\theta,\theta')\cdot\overline{I}^{me}(\theta',z) \quad (15a)$$

$$\cos\theta\frac{d}{dz}\overline{I}^{mo}(\theta,z) = -K_a\overline{I}^{mo}(\theta,z) - \overline{\overline{K}}_s(\theta)\cdot\overline{I}^{mo}(\theta,z)$$
$$+ \int_0^\pi d\theta'\sin\theta'\overline{\overline{P}}^{mo}(\theta,\theta')\cdot\overline{I}^{mo}(\theta',z) \quad (15b)$$

where

$$
\overline{\overline{P}}^{me}(\theta,\theta') =
\begin{bmatrix}
P_{11}^{mc} & P_{12}^{mc} & -P_{13}^{ms} & -P_{14}^{ms} \\
P_{21}^{mc} & P_{22}^{mc} & -P_{23}^{ms} & -P_{24}^{ms} \\
P_{31}^{ms} & P_{32}^{ms} & P_{33}^{mc} & P_{34}^{mc} \\
P_{41}^{ms} & P_{42}^{ms} & P_{43}^{mc} & P_{44}^{mc}
\end{bmatrix}
\tag{16a}
$$

$$
\overline{\overline{P}}^{mo}(\theta,\theta') =
\begin{bmatrix}
P_{11}^{mc} & P_{12}^{mc} & P_{13}^{ms} & P_{14}^{ms} \\
P_{21}^{mc} & P_{22}^{mc} & P_{23}^{ms} & P_{24}^{ms} \\
P_{31}^{ms} & P_{32}^{ms} & P_{33}^{mc} & P_{34}^{mc} \\
P_{41}^{ms} & P_{42}^{ms} & P_{43}^{mc} & P_{44}^{mc}
\end{bmatrix}
\tag{16b}
$$

In order to derive the boundary conditions for the Fourier-series expanded intensities, we first expand the incident intensity $\overline{I}_{oi}(\pi - \theta_o, \phi_{oi})$ into the Fourier series:

$$
\overline{I}_{oi}(\pi - \theta_o, \phi_o) = \overline{I}_{oi}\,\delta(\cos\theta_o - \cos\theta_{oi})\,\delta(\phi_o - \phi_{oi})
$$

$$
= \overline{I}_{oi}\,\delta(\cos\theta_o - \cos\theta_{oi}) \sum_{m=0}^{\infty} \frac{1}{(\delta_m + 1)\pi} \cos m(\phi_o - \phi_{oi})
\tag{17}
$$

Substituting the above equation along with the Fourier-series expanded intensities into the boundary conditions in (4) and (5) and collecting terms with the same azimuthal dependence, the boundary conditions for each harmonic can be obtained. The results are, for $\alpha = e$ or o, and $0 < \theta < \pi/2$, at $z = 0$

$$
\overline{I}^{m\alpha}(\pi - \theta, z = 0) = \overline{\overline{T}}_{01}(\theta_o) \cdot \overline{I}_{oi}^{m\alpha}(\pi - \theta_o) + \overline{\overline{R}}_{10}(\theta) \cdot \overline{I}^{m\alpha}(\theta, z = 0)
\tag{18}
$$

and at $z = -d$

$$
\overline{I}^{m\alpha}(\theta, z = -d) = \overline{\overline{R}}_{12}(\theta) \cdot \overline{I}^{m\alpha}(\pi - \theta, z = -d)
\tag{19}
$$

where

$$
\overline{I}_{oi}^{m\alpha}(\pi - \theta_o) = \overline{I}_{oi}^{m\alpha} \frac{1}{(\delta_m + 1)\pi}\,\delta(\cos\theta_o - \cos\theta_{oi})
\tag{20}
$$

with

$$
\overline{I}_{oi}^{me} =
\begin{bmatrix}
I_{vi} \\
I_{hi} \\
0 \\
0
\end{bmatrix}
\tag{21a}
$$

$$\overline{I}_{oi}^{mo} = \begin{bmatrix} 0 \\ 0 \\ U_i \\ V_i \end{bmatrix} \tag{21b}$$

We define m_{max} to be the number of harmonics that has to be kept in the expansion of the scattering function matrix such that

$$\overline{\overline{P}}^{mc}(\theta, \theta') \simeq \overline{\overline{P}}^{ms}(\theta, \theta') \simeq 0 \qquad \text{for} \quad m > m_{max} \tag{22}$$

Then, for $m > m_{max}$ the radiative transfer equations simplify to

$$\cos\theta \frac{d}{dz} \overline{I}^{me}(\theta, z) = -K_a \overline{I}^{me} - \overline{\overline{K}}_s(\theta) \cdot \overline{I}^{me}(\theta, z) \tag{23a}$$

$$\cos\theta \frac{d}{dz} \overline{I}^{mo}(\theta, z) = -K_a \overline{I}^{mo} - \overline{\overline{K}}_s(\theta) \cdot \overline{I}^{mo}(\theta, z) \tag{23b}$$

and the solutions to these equations can be obtained analytically, without resorting to the numerical approach.

c. Gaussian Quadrature Method

The set of decoupled radiative transfer equations without the azimuthal dependence for each harmonic can be solved numerically using the Gaussian quadrature method. The integrals in the radiative transfer equations are replaced by a Gaussian quadrature, an appropriately weighted sum over $2n$ intervals between $2n$ zeroes of the even-order Legendre polynomial $P_{2n}(\theta)$. The resulting system of $8n$ first-order differential equations are solved by obtaining eigenvalues and eigenvectors and matching the boundary conditions. In obtaining the eigenvalues and eigenvectors, the order of system of equations can be reduced by a factor of two to $4n$ equations by making use of the symmetry properties of the scattering function matrix and noting that the eigenvalues occur in pairs such that if ξ is an eigenvalue, so is $-\xi$. We first break up the radiative transfer equations into two set of equations by defining, for $\alpha = e, \beta = o$ or $\alpha = o, \beta = e$, and $m = 0, 1, 2, \cdots$

$$\overline{I}_1(\theta, z) \equiv \begin{bmatrix} I_{1_1}(\theta, z) \\ I_{1_2}(\theta, z) \end{bmatrix} = \begin{bmatrix} I_v^{m\alpha}(\theta, z) \\ I_h^{m\alpha}(\theta, z) \end{bmatrix} \tag{24a}$$

$$\overline{I}_2(\theta, z) \equiv \begin{bmatrix} I_{2_1}(\theta, z) \\ I_{2_2}(\theta, z) \end{bmatrix} = \begin{bmatrix} U^{m\beta}(\theta, z) \\ V^{m\beta}(\theta, z) \end{bmatrix} \tag{24b}$$

$$\overline{\overline{P}}_{11}(\theta, \theta') \equiv \begin{bmatrix} P_{11_{11}} & P_{11_{12}} \\ P_{11_{21}} & P_{11_{22}} \end{bmatrix} = \begin{bmatrix} P_{11}^{m\alpha} & P_{12}^{m\alpha} \\ P_{21}^{m\alpha} & P_{22}^{m\alpha} \end{bmatrix} \tag{25a}$$

$$\overline{\overline{P}}_{12}(\theta, \theta') \equiv \begin{bmatrix} P_{12_{11}} & P_{12_{12}} \\ P_{12_{21}} & P_{12_{22}} \end{bmatrix} = \begin{bmatrix} P_{13}^{m\alpha} & P_{14}^{m\alpha} \\ P_{23}^{m\alpha} & P_{24}^{m\alpha} \end{bmatrix} \tag{25b}$$

$$\overline{\overline{P}}_{21}(\theta, \theta') \equiv \begin{bmatrix} P_{21_{11}} & P_{21_{12}} \\ P_{21_{21}} & P_{21_{22}} \end{bmatrix} = \begin{bmatrix} P_{31}^{m\alpha} & P_{32}^{m\alpha} \\ P_{41}^{m\alpha} & P_{42}^{m\alpha} \end{bmatrix} \tag{25c}$$

$$\overline{\overline{P}}_{22}(\theta, \theta') \equiv \begin{bmatrix} P_{22_{11}} & P_{22_{12}} \\ P_{22_{21}} & P_{22_{22}} \end{bmatrix} = \begin{bmatrix} P_{33}^{m\alpha} & P_{34}^{m\alpha} \\ P_{43}^{m\alpha} & P_{44}^{m\alpha} \end{bmatrix} \tag{25d}$$

We then have

$$\cos\theta \frac{d}{dz}\overline{I}_1(\theta, z) = -\overline{\overline{K}}_{e1}(\theta) + \int_0^\pi d\theta' \sin\theta'$$
$$\times \left[\overline{\overline{P}}_{11}(\theta, \theta') \cdot \overline{I}_1(\theta', z) + \overline{\overline{P}}_{12}(\theta, \theta') \cdot \overline{I}_2(\theta', z)\right] \tag{26a}$$

$$\cos\theta \frac{d}{dz}\overline{I}_2(\theta, z) = -\overline{\overline{K}}_{e2}(\theta) + \int_0^\pi d\theta' \sin\theta'$$
$$\times \left[\overline{\overline{P}}_{21}(\theta, \theta') \cdot \overline{I}_1(\theta', z) + \overline{\overline{P}}_{22}(\theta, \theta') \cdot \overline{I}_2(\theta', z)\right] \tag{26b}$$

where

$$\overline{\overline{K}}_{e1}(\theta) = K_a + \overline{\overline{K}}_{s1} \tag{27a}$$

$$\overline{\overline{K}}_{e2}(\theta) = K_a + \overline{\overline{K}}_{s2} \tag{27b}$$

with

$$\overline{\overline{K}}_{s1} = \begin{bmatrix} K_v & 0 \\ 0 & K_h \end{bmatrix} \tag{28a}$$

$$\overline{\overline{K}}_{s2} = \begin{bmatrix} \frac{K_v + K_h}{2} & 0 \\ 0 & \frac{K_v + K_h}{2} \end{bmatrix} \tag{28b}$$

The scattering function matrix can be shown to satisfy the following properties. For $\alpha, \beta = 1$ or 2,

$$\overline{\overline{P}}_{\alpha\alpha}(\theta, \theta') = \overline{\overline{P}}_{\alpha\alpha}(\pi - \theta, \pi - \theta') \tag{29a}$$

$$\overline{\overline{P}}_{\alpha\alpha}(\pi - \theta, \theta') = \overline{\overline{P}}_{\alpha\alpha}(\theta, \pi - \theta') \tag{29b}$$

and for $\alpha \neq \beta$

$$\overline{\overline{P}}_{\alpha\beta}(\theta, \theta') = -\overline{\overline{P}}_{\alpha\beta}(\pi - \theta, \pi - \theta') \tag{30a}$$

$$\overline{\overline{P}}_{\alpha\beta}(\pi - \theta, \theta') = -\overline{\overline{P}}_{\alpha\beta}(\theta, \pi - \theta') \tag{30b}$$

Further breaking up the intensities into upward and downward propagating intensities, denoted by superscripts $+$ and $-$, respectively, and applying the Gaussian quadrature method, we obtain the following set of equations by making use of the symmetry properties of the scattering function matrix:

$$\overline{\overline{\mu}} \cdot \frac{d}{dz} \overline{I}_1^+ = -\overline{\overline{K}}_{e1} \cdot \overline{I}_1^+ + \overline{\overline{F}}_{11} \cdot \overline{I}_1^+ + \overline{\overline{B}}_{11} \cdot \overline{I}_1^- + \overline{\overline{F}}_{12} \cdot \overline{I}_2^+ + \overline{\overline{B}}_{12} \cdot \overline{I}_2^-$$

$$\tag{31a}$$

$$-\overline{\overline{\mu}} \cdot \frac{d}{dz} \overline{I}_1^- = -\overline{\overline{K}}_{e1} \cdot \overline{I}_1^- + \overline{\overline{B}}_{11} \cdot \overline{I}_1^+ + \overline{\overline{F}}_{11} \cdot \overline{I}_1^- - \overline{\overline{B}}_{12} \cdot \overline{I}_2^+ - \overline{\overline{F}}_{12} \cdot \overline{I}_2^-$$

$$\tag{31b}$$

$$\overline{\overline{\mu}} \cdot \frac{d}{dz} \overline{I}_2^+ = -\overline{\overline{K}}_{e2} \cdot \overline{I}_2^+ + \overline{\overline{F}}_{21} \cdot \overline{I}_1^+ + \overline{\overline{B}}_{21} \cdot \overline{I}_1^- + \overline{\overline{F}}_{22} \cdot \overline{I}_2^+ + \overline{\overline{B}}_{22} \cdot \overline{I}_2^-$$

$$\tag{32a}$$

$$-\overline{\overline{\mu}} \cdot \frac{d}{dz} \overline{I}_2^- = -\overline{\overline{K}}_{e2} \cdot \overline{I}_2^- - \overline{\overline{B}}_{21} \cdot \overline{I}_1^+ - \overline{\overline{F}}_{21} \cdot \overline{I}_1^- + \overline{\overline{B}}_{22} \cdot \overline{I}_2^+ + \overline{\overline{F}}_{22} \cdot \overline{I}_2^-$$

$$\tag{32b}$$

where, for $\alpha, \beta = 1, 2$, I_α^+ and I_α^- are $2n \times 1$ matrices

$$\overline{I}_\alpha^+ = \begin{bmatrix} I_{\alpha_1}(\mu_1, z) \\ \vdots \\ I_{\alpha_1}(\mu_n, z) \\ I_{\alpha_2}(\mu_1, z) \\ \vdots \\ I_{\alpha_2}(\mu_n, z) \end{bmatrix} \qquad \overline{I}_\alpha^- = \begin{bmatrix} I_{\alpha_1}(-\mu_1, z) \\ \vdots \\ I_{\alpha_1}(-\mu_n, z) \\ I_{\alpha_2}(-\mu_1, z) \\ \vdots \\ I_{\alpha_2}(-\mu_n, z) \end{bmatrix} \tag{33}$$

and $\overline{\overline{F}}_{\alpha\beta}$ and $\overline{\overline{B}}_{\alpha\beta}$ are the $2n \times 2n$ matrices

$$\overline{\overline{F}}_{\alpha\beta} = \begin{bmatrix} P_{\alpha\beta_{11}}(\mu_1,\mu_1) & \cdots & P_{\alpha\beta_{11}}(\mu_1,\mu_n) & P_{\alpha\beta_{12}}(\mu_1,\mu_1) & \cdots & P_{\alpha\beta_{12}}(\mu_1,\mu_n) \\ \vdots & \vdots & \vdots & \vdots & \vdots & \vdots \\ P_{\alpha\beta_{11}}(\mu_n,\mu_1) & \cdots & P_{\alpha\beta_{11}}(\mu_n,\mu_n) & P_{\alpha\beta_{12}}(\mu_n,\mu_1) & \cdots & P_{\alpha\beta_{12}}(\mu_n,\mu_n) \\ P_{\alpha\beta_{21}}(\mu_1,\mu_1) & \cdots & P_{\alpha\beta_{21}}(\mu_1,\mu_n) & P_{\alpha\beta_{22}}(\mu_1,\mu_1) & \cdots & P_{\alpha\beta_{22}}(\mu_1,\mu_n) \\ \vdots & \vdots & \vdots & \vdots & \vdots & \vdots \\ P_{\alpha\beta_{21}}(\mu_n,\mu_1) & \cdots & P_{\alpha\beta_{21}}(\mu_n,\mu_n) & P_{\alpha\beta_{22}}(\mu_n,\mu_1) & \cdots & P_{\alpha\beta_{22}}(\mu_n,\mu_n) \end{bmatrix}$$

$$(34)$$

$$\overline{\overline{B}}_{\alpha\beta} = \begin{bmatrix} P_{\alpha\beta_{11}}(\mu_1,-\mu_1) & \cdots & P_{\alpha\beta_{11}}(\mu_1,-\mu_n) & P_{\alpha\beta_{12}}(\mu_1,-\mu_1) & \cdots & P_{\alpha\beta_{12}}(\mu_1,-\mu_n) \\ \vdots & \vdots & \vdots & \vdots & \vdots & \vdots \\ P_{\alpha\beta_{11}}(\mu_n,-\mu_1) & \cdots & P_{\alpha\beta_{11}}(\mu_n,-\mu_n) & P_{\alpha\beta_{12}}(\mu_n,-\mu_1) & \cdots & P_{\alpha\beta_{12}}(\mu_n,-\mu_n) \\ P_{\alpha\beta_{21}}(\mu_1,-\mu_1) & \cdots & P_{\alpha\beta_{21}}(\mu_1,-\mu_n) & P_{\alpha\beta_{22}}(\mu_1,-\mu_1) & \cdots & P_{\alpha\beta_{22}}(\mu_1,-\mu_n) \\ \vdots & \vdots & \vdots & \vdots & \vdots & \vdots \\ P_{\alpha\beta_{21}}(\mu_n,-\mu_1) & \cdots & P_{\alpha\beta_{21}}(\mu_n,-\mu_n) & P_{\alpha\beta_{22}}(\mu_n,-\mu_1) & \cdots & P_{\alpha\beta_{22}}(\mu_n,-\mu_n) \end{bmatrix}$$

$$(35)$$

and $\overline{\overline{\mu}}$ and $\overline{\overline{a}}$ are the $2n \times 2n$ diagonal matrices

$$\overline{\overline{\mu}} = \text{diag}[\mu_1, \cdots, \mu_n, \mu_1, \cdots, \mu_n] \tag{36}$$

$$\overline{\overline{a}} = \text{diag}[a_1, \cdots, a_n, a_1, \cdots, a_n] \tag{37}$$

In the above equation $\pm\mu_i$ are the zeroes of the Legendre polynomial $P_{2n}(\mu)$ and a_i are the corresponding Christoffel weighting functions and we made use of the relations $a_i = a_{-i}$ and $\mu_i = -\mu_{-i}$.

The system of $8n$ first-order differential equations, (31) and (32), can be cast into more compact form by defining $4n \times 1$ matrices $\overline{I}_a$ and $\overline{I}_s$

$$\overline{I}_a = \begin{bmatrix} \overline{I}_{a1} \\ \overline{I}_{s2} \end{bmatrix} \qquad \overline{I}_s = \begin{bmatrix} \overline{I}_{s1} \\ \overline{I}_{a2} \end{bmatrix} \tag{38}$$

such that upward propagating intensity $\overline{I}^+$ is given by

$$\overline{I}^+ \equiv \begin{bmatrix} \overline{I}_1^+ \\ \overline{I}_2^+ \end{bmatrix} = \frac{1}{2}[\overline{I}_a + \overline{I}_s] \tag{39}$$

and where, for $l = 1, 2$, $\bar{I}_{al} = \bar{I}_l^+ + \bar{I}_l^-$ and $\bar{I}_{sl} = \bar{I}_l^+ - \bar{I}_l^-$. Then, from (31) and (32), we obtain

$$\bar{\bar{\mu}} \cdot \frac{d}{dz} \bar{I}_a = \bar{\bar{W}} \cdot \bar{I}_s \tag{40a}$$

$$\bar{\bar{\mu}} \cdot \frac{d}{dz} \bar{I}_s = \bar{\bar{A}} \cdot \bar{I}_a \tag{40b}$$

where $\bar{\bar{W}}$ and $\bar{\bar{A}}$ are the $4n \times 4n$ matrices

$$\bar{\bar{W}} = - \begin{bmatrix} \bar{\bar{K}}_{e1} & 0 \\ 0 & \bar{\bar{K}}_{e2} \end{bmatrix} + \begin{bmatrix} (\bar{\bar{F}}_{11} - \bar{\bar{B}}_{11}) & (\bar{\bar{F}}_{12} + \bar{\bar{B}}_{12}) \\ (\bar{\bar{F}}_{21} - \bar{\bar{B}}_{21}) & (\bar{\bar{F}}_{22} + \bar{\bar{B}}_{22}) \end{bmatrix} \cdot \bar{\bar{a}} \tag{41a}$$

$$\bar{\bar{A}} = - \begin{bmatrix} \bar{\bar{K}}_{e1} & 0 \\ 0 & \bar{\bar{K}}_{e2} \end{bmatrix} + \begin{bmatrix} (\bar{\bar{F}}_{11} + \bar{\bar{B}}_{11}) & (\bar{\bar{F}}_{12} - \bar{\bar{B}}_{12}) \\ (\bar{\bar{F}}_{21} + \bar{\bar{B}}_{21}) & (\bar{\bar{F}}_{22} - \bar{\bar{B}}_{22}) \end{bmatrix} \cdot \bar{\bar{a}} \tag{41b}$$

and the $\bar{\bar{\mu}}$ and $\bar{\bar{a}}$ are $4n \times 4n$ diagonal matrices

$$\bar{\bar{\mu}} = \mathrm{diag}[\mu_1, \cdots, \mu_n, \mu_1, \cdots, \mu_n, \mu_1, \cdots, \mu_n, \mu_1, \cdots, \mu_n] \tag{42a}$$

$$\bar{\bar{a}} = \mathrm{diag}[a_1, \cdots, a_n, a_1, \cdots, a_n, a_1, \cdots, a_n, a_1, \cdots, a_n] \tag{42b}$$

The homogeneous solution can be obtained in the form

$$\bar{I}_a = \bar{I}_{ao} e^{\alpha z} \tag{43a}$$

$$\bar{I}_s = \bar{I}_{so} e^{\alpha z} \tag{43b}$$

Substituting the above equations into (40a) and (40b), we now have $4n$ eigenvalue equations.

$$(\bar{\bar{\mu}}^{-1} \cdot \bar{\bar{W}} \cdot \bar{\bar{\mu}}^{-1} \cdot \bar{\bar{A}} - \alpha^2 \bar{\bar{I}}) \cdot \bar{I}_{ao} = 0 \tag{44}$$

$$\bar{I}_{so} = \alpha^{-1} \bar{\bar{\mu}}^{-1} \cdot \bar{\bar{A}} \cdot \bar{I}_{ao} \tag{45}$$

where $\bar{\bar{I}}$ is an identity matrix. Thus, if α is an eigenvalue, so is $-\alpha$. Once the eigenvalues α_i and the corresponding eigenvectors $\bar{I}_{ai}$ are obtained, we let $\bar{\bar{E}} = (\bar{I}_{a_1}, \bar{I}_{a_2}, \cdots, \bar{I}_{a_{4n}})$ be the $4n \times 4n$ eigenmatrix. Then the total solution for the upward propagating intensity is given by

$$\bar{I}^+ = (\bar{\bar{E}} + \bar{\bar{Q}}) \cdot \bar{\bar{D}}(z) \cdot \bar{x} + (\bar{\bar{E}} - \bar{\bar{Q}}) \cdot \bar{\bar{U}}(z + d) \cdot \bar{y} \tag{46}$$

where

$$\overline{\overline{Q}} = \overline{\overline{\mu}}^{-1} \cdot \overline{\overline{A}} \cdot \overline{\overline{E}} \cdot \overline{\overline{\alpha}}^{-1} \tag{47}$$

$$\overline{\overline{\alpha}} = \text{diag}[\alpha_1, \alpha_2, \cdots, \alpha_{4n}] \tag{48}$$

$$\overline{\overline{D}}(z) = \text{diag}\left[e^{\alpha_1 z}, e^{\alpha_2 z}, \cdots, e^{\alpha_{4n} z}\right] \tag{49}$$

$$\overline{\overline{U}}(z) = \text{diag}\left[e^{-\alpha_1 z}, e^{-\alpha_2 z}, \cdots, e^{-\alpha_{4n} z}\right] \tag{50}$$

and $\overline{x}$ and $\overline{y}$ are the $4n \times 1$ matrices which represent $8n$ unknowns to be determined by the boundary conditions.

In a similar manner, the downward propagating intensity $\overline{I}^-$ can calculated. We obtain,

$$\overline{I}^- = (\overline{\overline{E}}' + \overline{\overline{Q}}') \cdot \overline{\overline{D}}(z) \cdot \overline{x} + (\overline{\overline{E}}' - \overline{\overline{Q}}') \cdot \overline{\overline{U}}(z+d) \cdot \overline{y} \tag{51}$$

where

$$\overline{\overline{E}}' = \overline{\overline{\mu}}^{-1} \cdot \overline{\overline{W}}' \cdot \overline{\overline{Q}} \cdot \overline{\overline{\alpha}}^{-1} \tag{52a}$$

$$\overline{\overline{Q}}' = \overline{\overline{\mu}}^{-1} \cdot \overline{\overline{A}}' \cdot \overline{\overline{E}} \cdot \overline{\overline{\alpha}}^{-1} \tag{52b}$$

and

$$\overline{\overline{W}}' = -\begin{bmatrix} \overline{\overline{K}}_{e1} & 0 \\ 0 & -\overline{\overline{K}}_{e2} \end{bmatrix} + \begin{bmatrix} (\overline{\overline{F}}_{11} - \overline{\overline{B}}_{11}) & (\overline{\overline{F}}_{12} + \overline{\overline{B}}_{12}) \\ -(\overline{\overline{F}}_{21} - \overline{\overline{B}}_{21}) & -(\overline{\overline{F}}_{22} + \overline{\overline{B}}_{22}) \end{bmatrix} \cdot \overline{\overline{a}} \tag{53a}$$

$$\overline{\overline{A}}' = -\begin{bmatrix} -\overline{\overline{K}}_{e1} & 0 \\ 0 & \overline{\overline{K}}_{e2} \end{bmatrix} + \begin{bmatrix} -(\overline{\overline{F}}_{11} + \overline{\overline{B}}_{11}) & -(\overline{\overline{F}}_{12} - \overline{\overline{B}}_{12}) \\ (\overline{\overline{F}}_{21} + \overline{\overline{B}}_{21}) & (\overline{\overline{F}}_{22} - \overline{\overline{B}}_{22}) \end{bmatrix} \cdot \overline{\overline{a}} \tag{53b}$$

In the random medium model, the eigenvalue equations can be simplified further since there is no coupling between the first three Stokes parameters, I_v, I_h, and U, and the last Stokes parameter V in the scattering function matrix. However, the Stokes parameters U and V are coupled together in the boundary conditions, and, in general, we have to keep all four Stokes parameters.

The boundary conditions, which are to be used to determine the constants $\overline{x}$ and $\overline{y}$ of the upward and downward propagating intensities given by (46) and (51), are, at $z = -d$,

$$\overline{I}^+(z = -d) = \overline{\overline{R}}_{12} \cdot \overline{I}^-(z = -d) \tag{54}$$

and at $z = 0$

$$\overline{I}^-(z = 0) = \overline{\overline{R}}_{10} \cdot \overline{I}^+(z = 0) + \overline{\overline{T}}_{01} \cdot \overline{I}_{oi}^- \tag{55}$$

where $\overline{\overline{R}}_{12}$ and $\overline{\overline{R}}_{10}$ are the $4n \times 4n$ matrices which are obtained by evaluating the 4×4 coupling matrices $\overline{\overline{R}}_{12}(\theta)$ and $\overline{\overline{R}}_{10}(\theta)$ at n discrete quadrature angles, and $\overline{\overline{T}}_{01}$ is the $4n \times 4n_f$ matrix which is obtained by evaluating the coupling matrix $\overline{\overline{T}}_{01}$ at the quadrature angles. The n_f is the number of quadrature angles in region 0, and the quadrature angles are related by the Snell's law. Since $\epsilon_1' \geq \epsilon_o$ we have $n_f \leq n$. Thus, for the quadrature angles in region 1 which are greater than the critical angle between regions 1 and 0, θ_i where $i > n_f$, there is no incident intensity. In the above equation (55), the incident intensity $\overline{I}_{oi}^-$ is obtained by discretizing the incident intensity given by (20), which is given in terms of the delta function. One way to bypass the problem of discretizing the delta function is to change the source term at the boundary into the source term in the volume by calculating the zeroth-order solution explicitly and using the radiative transfer equations for the higher order terms with the zeroth-order solution acting as the volume source [51]. In this section we discretize the delta function in a consistent manner and keep the source term at the boundary. This approach gives the same solution as the other approach, and also the formulation does not have to be changed when the boundary conditions are changed to incorporate the rough surface scattering [51].

Consider an integral given by

$$I = \int_0^\pi d\theta' \, \sin\theta' f(\theta, \theta') g(\theta') \tag{56}$$

Using the Gaussian quadrature method the integral I is approximated as

$$I \simeq \sum_{j=-n}^{n} a_j \, f(\theta, \theta_j) \, g_j \tag{57}$$

If we now let $g(\theta') = \delta(\cos\theta_o' - \cos\theta_{oi})$ where θ_{oi} is one of the quadrature angles in region 0, then the integral I can be evaluated exactly to give

$$I = f(\theta, \theta_i) \frac{\epsilon_o}{\epsilon_1'} \frac{\cos\theta_{oi}}{\cos\theta_i} \tag{58}$$

where θ_i is the corresponding incident angle in region 1 which is related to θ_{oi} by Snell's law, and we made use of [40]

$$d\theta' \sin \theta' d\phi' = d\theta'_o \sin \theta'_o \frac{\epsilon_o}{\epsilon'_1} \frac{\cos \theta_{oi}}{\cos \theta_i} \, d\phi'_o \qquad (59)$$

Therefore, comparing (58) with (57), we obtain the discrete form for the delta function:

$$g_j = \delta_{ji} \frac{1}{a_j} \frac{\epsilon_o}{\epsilon'_1} \frac{\cos \theta_{oi}}{\cos \theta_i} \qquad (60)$$

where

$$\delta_{ji} = \begin{cases} 1 & \text{if } j = i \\ 0 & \text{otherwise} \end{cases} \qquad (61)$$

The incident intensities for even and odd terms in each harmonic, given by (20), can now be cast into the quadrature form by making use of the above relations.

Substituting in the expressions for the upward and downward propagating intensities into the boundary conditions (54) and (55), we obtain the following $8n$ equations for $8n$ unknowns $\bar{x}$ and $\bar{y}$:

$$\left[(\overline{\overline{E}}' + \overline{\overline{Q}}') - \overline{\overline{R}}_{10} \cdot (\overline{\overline{E}} + \overline{\overline{Q}}) \right] \cdot \bar{x}$$
$$+ \left[(\overline{\overline{E}}' - \overline{\overline{Q}}') - \overline{\overline{R}}_{10} \cdot (\overline{\overline{E}} - \overline{\overline{Q}}) \right] \cdot \overline{\overline{D}}(-d) \cdot \bar{y} = \overline{\overline{T}}_{01} \cdot \overline{I}_{oi}^{-} \qquad (62a)$$

$$\left[(\overline{\overline{E}} + \overline{\overline{Q}}) - \overline{\overline{R}}_{12} \cdot (\overline{\overline{E}}' + \overline{\overline{Q}}') \right] \cdot \overline{\overline{D}}(-d) \cdot \bar{x}$$
$$+ \left[(\overline{\overline{E}} - \overline{\overline{Q}}) - \overline{\overline{R}}_{12} \cdot (\overline{\overline{E}}' - \overline{\overline{Q}}') \right] \cdot \bar{y} = 0 \qquad (62b)$$

The above equations can be solved for the constants $\bar{x}$ and $\bar{y}$ for each case when the incident intensity is at one of the quadrature angles. Note that in the halfspace random medium case when $d \to \infty$, the equations for $\bar{x}$ and $\bar{y}$ become decoupled since $\overline{\overline{D}} \to 0$ and the matrix equation does not become singular [51]. This is due to the form of the solution assumed in (46) and (51).

Once the constants $\bar{x}$ and $\bar{y}$ are determined, the scattered intensities from region 1 to region 0, represented by the first term on the right-hand-side of (6), can be determined. We have

$$\overline{I}_{os} = \overline{\overline{T}}_{10} \cdot \overline{I}^{+}(z = 0)$$

$$= \overline{\overline{T}}_{10} \cdot \left[(\overline{\overline{E}} + \overline{\overline{Q}}) \cdot \bar{x} + (\overline{\overline{E}} - \overline{\overline{Q}}) \cdot \overline{\overline{D}}(-d) \cdot \bar{y} \right] \qquad (63)$$

Thus, the complete solution can be obtained by solving the radiative transfer equations using the Gaussian quadrature method for each harmonic as outlined above and reintroducing the azimuthal dependence. The total scattered intensities in region 0 is given by

$$
\bar{I}_{os}(\phi_o) = \left\{ \bar{\bar{R}}_{01} + \bar{\bar{T}}_{10} \cdot \left[\bar{\bar{I}} - \bar{\bar{R}}_{10} \cdot \bar{\bar{R}}_{12} \cdot \exp[-\bar{\bar{\mu}}^{-1} \cdot \bar{\bar{K}}_e d] \right]^{-1} \cdot \bar{\bar{T}}_{01} \right\}
$$

$$
\cdot \bar{I}_{oi}\, \delta(\phi_o - \phi_{oi}) + \sum_{m=0}^{m_{mas}} \left\{ \bar{\bar{T}}_{10} \cdot \left[\bar{I}^{mc^+}(z=0) \right. \right.
$$

$$
- \left[\bar{\bar{I}} - \bar{\bar{R}}_{10} \cdot \bar{\bar{R}}_{12} \cdot \exp[-\mu^{-1} \cdot \bar{\bar{K}}_e d] \right]^{-1} \cdot \bar{\bar{T}}_{01}\, \bar{I}_{oi}^{mc} \right]
$$

$$
\cdot \cos m(\phi_o - \phi_{oi}) + \bar{\bar{T}}_{10} \cdot \bar{I}^{ms^+}(z=0) \sin m(\phi_o - \phi_{oi}) \right\} \tag{64}
$$

where we have summed up the zeroth-order solution and $\bar{I}^{mc^+}(z = 0)$ and $\bar{I}^{ms^+}(z = 0)$ are the upward propagating m-th cosine and sine harmonics evaluated at $z = 0$. Once the scattered intensities in region 0 are obtained, the bistatic scattering coefficients and the backscattering cross sections can be obtained from (7) and (8). Note that if we are interested in calculating the scattering intensities for vertically or horizontally polarized intensities only, then the even series needs to be calculated. This is because the odd series, represented by (14b), is zero due to the fact the incident intensity for the odd series as given by (21b) is zero. In general, both the even and odd series have to be calculated, especially for fully polarimetric scattering calculations.

d. Results and Discussion

The backscattering cross sections and the bistatic scattering coefficients are calculated and illustrated for the various cases. In our calculations $n = 16$ is used. The backscattering cross sections are illustrated as functions of frequency and incident angle. The bistatic scattering coefficients are plotted as functions of scattering angles θ_s and ϕ_s.

In Fig. 5.2.2 the horizontally polarized and depolarized backscattering cross sections are plotted as a function of frequency for a 48cm thick random medium. Backscattering cross sections increase as frequency is increased. This is due to the fact that as frequency increases
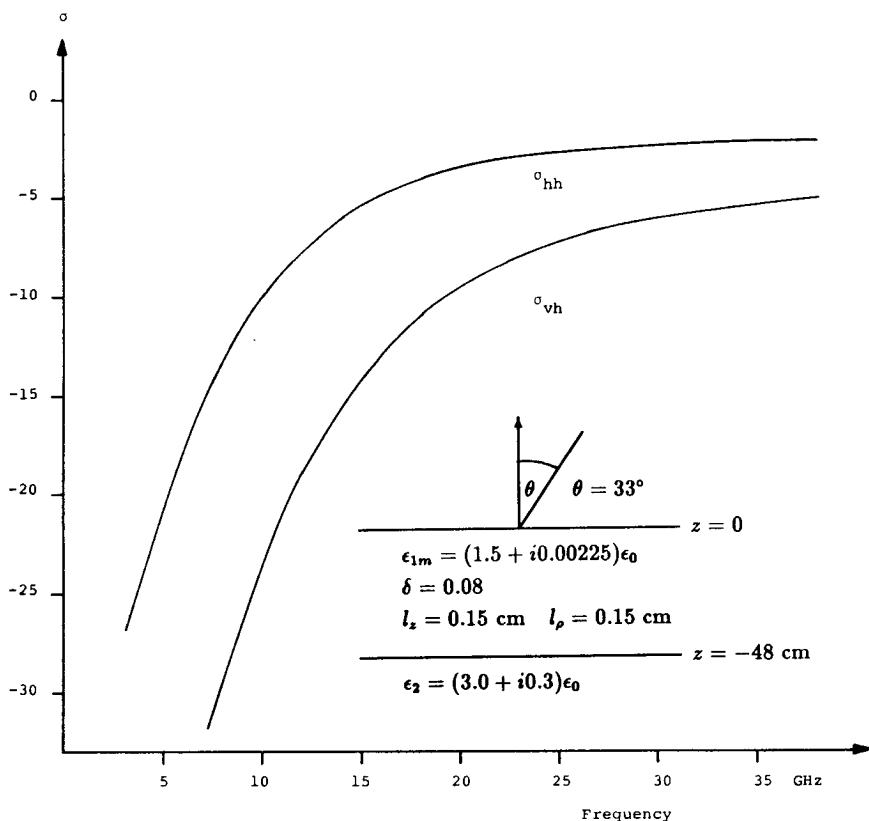
Figure 5.2.2 Backscattering cross sections as a function of frequency.

the albedo $[K_s/(K_a+K_s)]$ increases, and the scattering becomes dominant over the absorption. Also, the difference between the like-like polarized return and the depolarized return decreases. In Fig. 5.2.3 the backscattering cross sections are plotted as a function of incident angle at 10 GHz.

In Fig. 5.2.4, the bistatic scattering coefficients γ_{hh} and γ_{vh} are plotted as a function of scattering angle θ_s. The positive θ_s corresponds to the forward scattering case where $\phi_s = 0$ whereas negative θ_s corresponds to the backward scattering case with $\phi_s = 180°$. We note that there is symmetry about the $\theta_s = 0$ axis which is typical of Rayleigh scatterers. For correlation lengths small compared to the wavelength, the scattering pattern of the random medium is that of the Rayleigh scatterers [37]. The number of harmonics needed in this
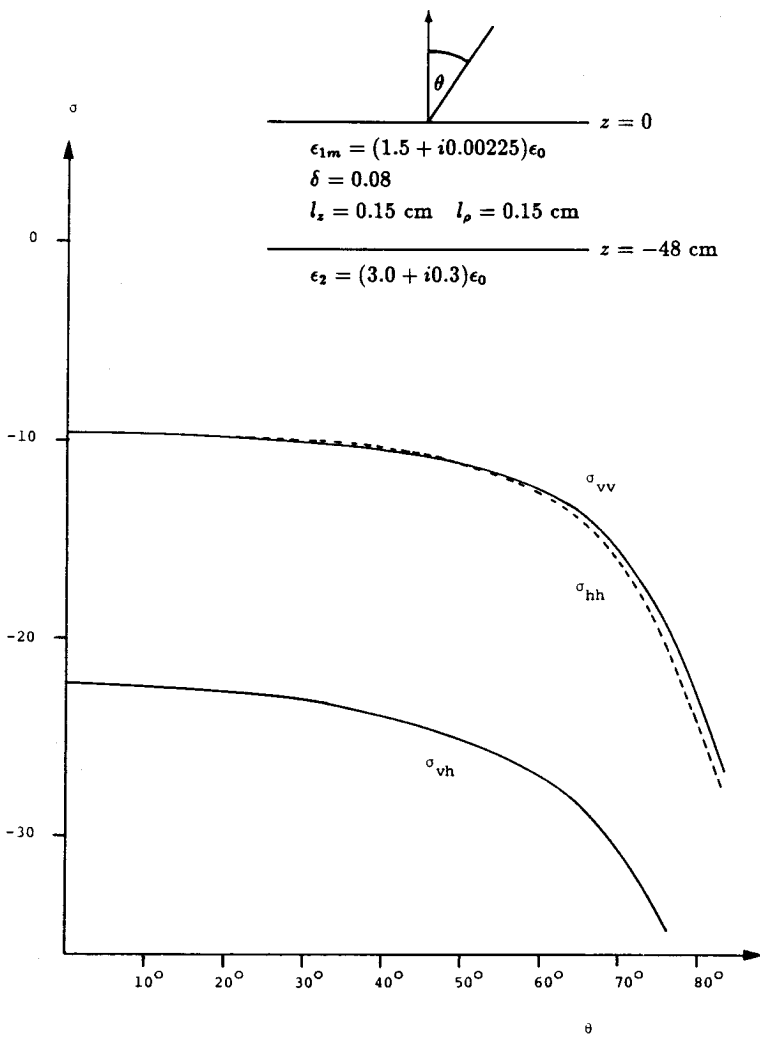
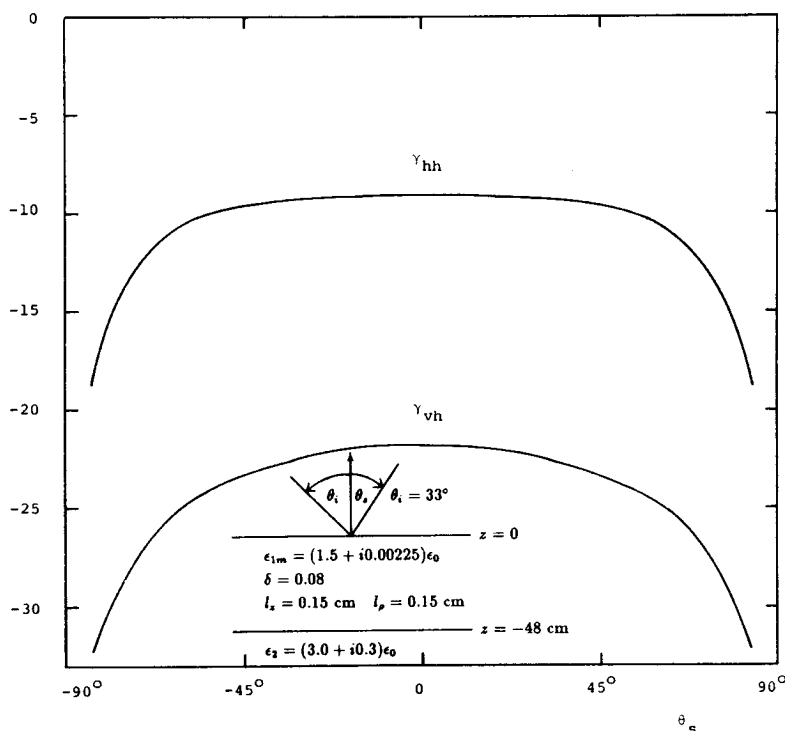**Figure 5.2.3 Backscattering cross sections as a function of incident angle at 10 GHz.**

Figure 5.2.4 **Bistatic scattering coefficients γ_{hh} and γ_{vh} as a function of scattering angle θ_s at 10 GHz.**

case was three which is the same as the case involving Rayleigh scatterers [53]. In Fig. 5.2.5 we show the bistatic scattering coefficients for the larger correlation length l_ρ. Unlike the previous case there is no symmetry. The number of harmonics needed in the computation is also larger than the previous case.
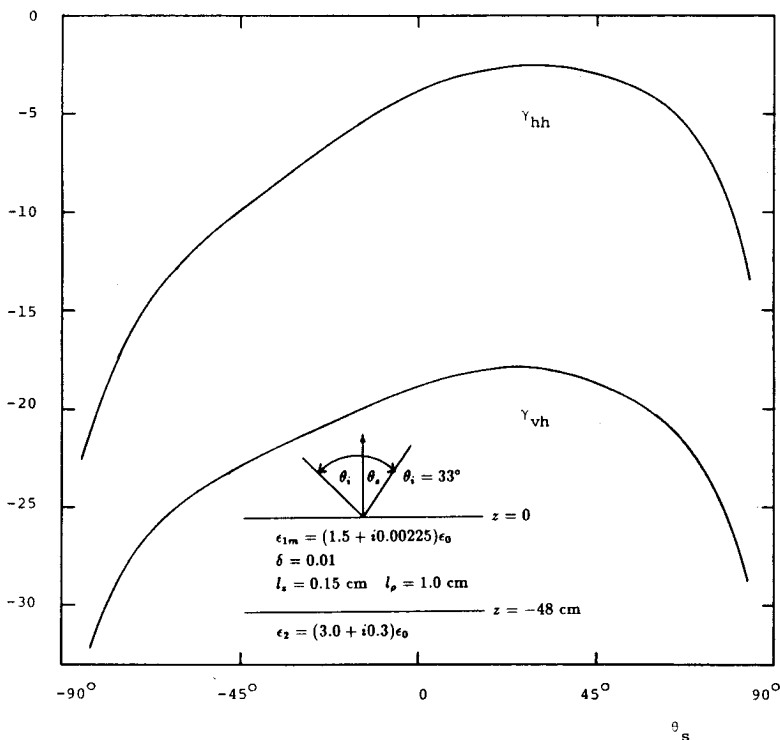
Figure 5.2.5 Bistatic scattering coefficients γ_{hh} and γ_{vh} as a function of scattering angle θ_s at 10 GHz.

In Figs. 5.2.6–5.2.9, the bistatic scattering coefficients are plotted as a function of azimuthal scattering angle ϕ_s for $\theta_i = \theta_s = 33°$. We only plot from $\phi_s = 0°$ to $\phi_s = 180°$ because the bistatc scattering coefficients are symmetrical. In Fig. 5.2.6, the bistatic scattering coefficients γ_{hh} and γ_{vh} are plotted for the case of small correlation length l_ρ. There is a symmetry in the bistatic scattering coefficients about $\phi_s = 90°$. In Fig. 5.2.7, γ_{hh} and γ_{vv} are compared. We note there is no symmetry for the bistatic scattering coefficient γ_{vv}. In Figs. 5.2.8 and 5.2.9, the bistatic scattering coefficients are plotted for the case of the large correlation length l_ρ. We note that the scattering coefficients are more peaked toward the forward scattering direction and that there is no symmetry about the $\phi_s = 90°$ axis.
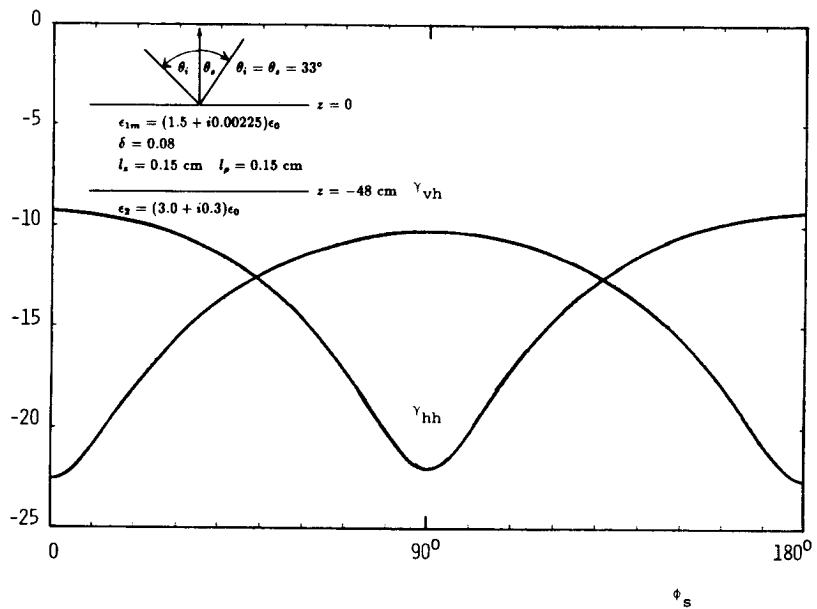
Figure 5.2.6 Bistatic scattering coefficients γ_{hh} and γ_{vh} as a function of azimuthal scattering angle ϕ_s at 10 GHz.
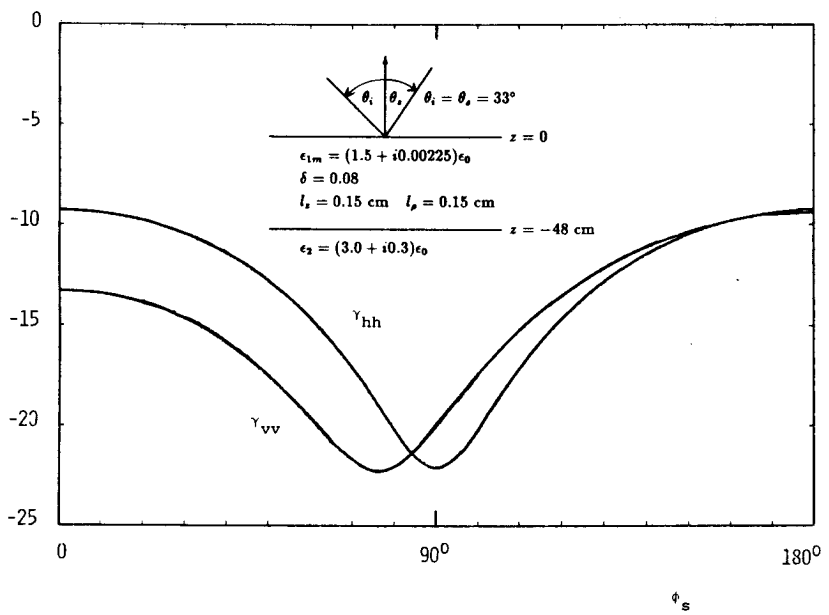
Figure 5.2.7 Bistatic scattering coefficients γ_{hh} and γ_{vh} as a function of azimuthal scattering angle ϕ_s at 10 GHz.
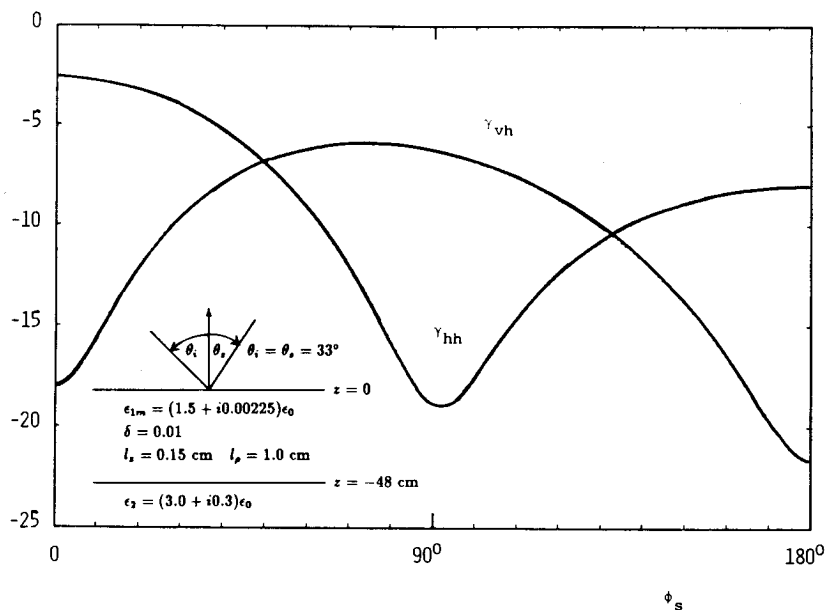
Figure 5.2.8 Bistatic scattering coefficients γ_{hh} and γ_{vh} as a function of azimuthal scattering angle ϕ_s at 10 GHz.
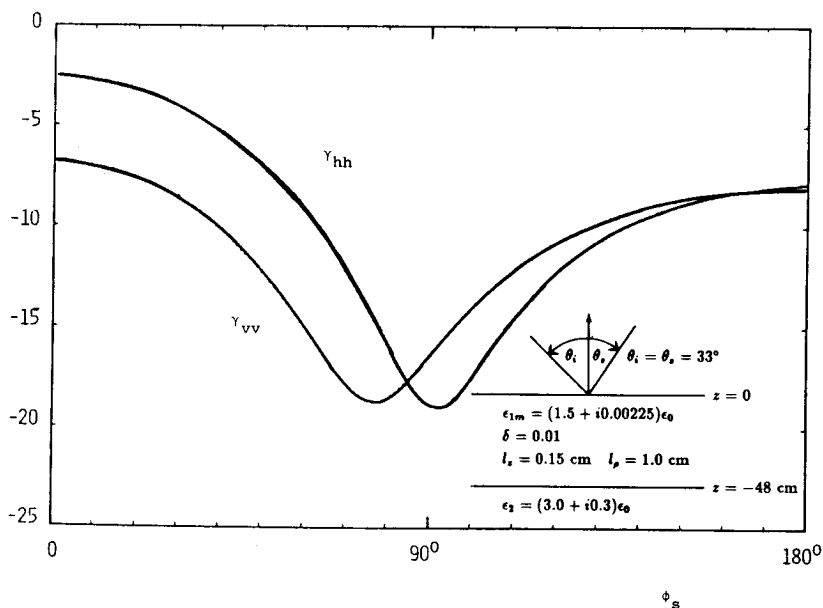
Figure 5.2.9 Bistatic scattering coefficients γ_{hh} and γ_{vh} as a function of azimuthal scattering angle ϕ_s at 10 GHz.

5.3 Two-Layer Random Medium with Rough Interfaces

a. Formulation

Consider a layer of random medium with rough interfaces characterized by the permittivity $\epsilon_1 + \epsilon_f$, where ϵ_f stands for the randomly fluctuating part whose amplitude is very small and whose ensemble average is zero, on top of a homogeneous medium with permittivity ϵ_2 [Fig. 5.3.1]. The radiative transfer equations which govern the propagation of intensities inside the scattering medium are given by (1) and (2).

For the case of rough interfaces, the boundary conditions are, for $0 < \theta < \pi/2$,

$$\bar{I}(\pi - \theta, \phi, z = 0)$$

$$= \int_0^{2\pi} d\phi_o' \int_0^{\pi/2} d\theta_o' \sin\theta_o' \; \overline{\overline{T}}_{01}(\theta, \phi; \theta_o', \phi_o') \cdot \bar{I}_{oi}(\pi - \theta_o', \phi_o')$$

$$+ \int_0^{2\pi} d\phi' \int_0^{\pi/2} d\theta' \sin\theta' \; \overline{\overline{R}}_{10}(\theta, \phi; \theta', \phi') \cdot \bar{I}(\theta', \phi', z = 0) \quad (65)$$

$$\bar{I}(\theta, \phi, z = -d)$$

$$= \int_0^{2\pi} d\phi' \int_0^{\pi/2} d\theta' \sin\theta' \; \overline{\overline{R}}_{12}(\theta, \phi; \theta', \phi') \cdot \bar{I}(\pi - \theta', \phi, z = -d) \quad (66)$$

where we have broken up the intensities in the scattering layer into upward going intensities $\bar{I}(\theta, \phi, z)$ and downward going intensities $\bar{I}(\pi - \theta, \phi, z)$, and $\bar{I}_{oi}(\pi - \theta_o, \phi_o)$ is the incident intensity given by (3). In the above equations $\overline{\overline{T}}_{01}(\theta, \phi; \theta_o, \phi_o)$ represents the coupling from region 0 to region 1, $\overline{\overline{R}}_{10}(\theta, \phi; \theta', \phi')$ represents the coupling from upward going intensity in the direction (θ', ϕ') into downward going intensity in the direction $(\pi - \theta, \phi)$ at the boundary of region 1 and region 0, and $\overline{\overline{R}}_{12}(\theta, \phi; \theta', \phi')$ represents similar coupling at the boundary of region 1 and region 2.

Once the radiative transfer equations are solved subject to the boundary conditions, the scattered intensity in the direction (θ_{os}, ϕ_{os}) in region 0 is determined from
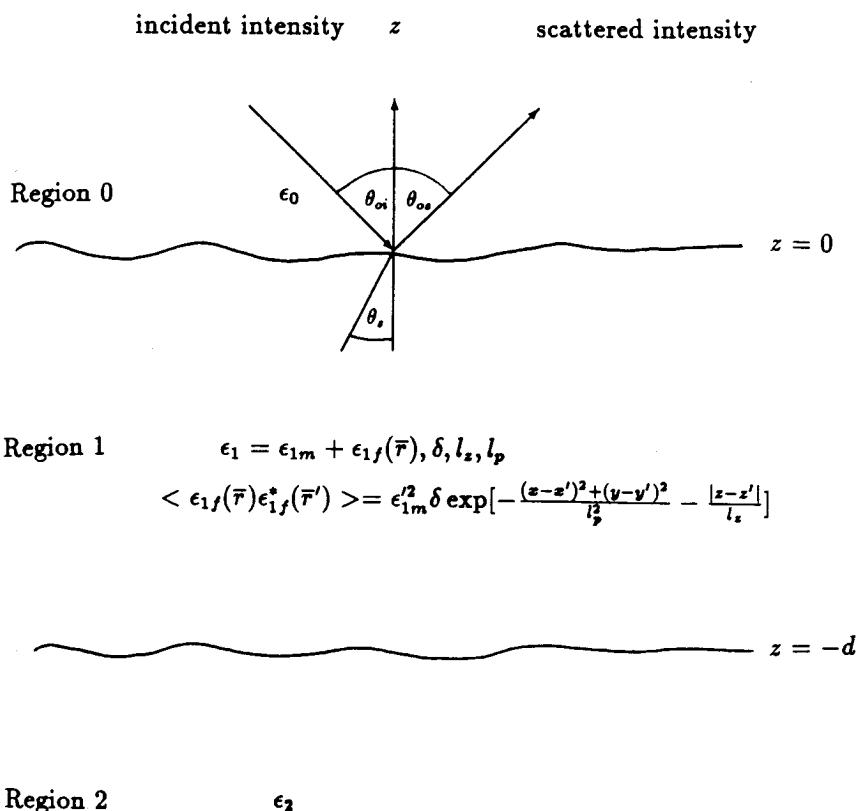
incident intensity $\quad z \quad$ scattered intensity

Region 0 $\qquad \epsilon_0$

θ_{oi} θ_{os}

$z = 0$

θ_s

Region 1 $\qquad \epsilon_1 = \epsilon_{1m} + \epsilon_{1f}(\bar{r}), \delta, l_z, l_p$

$$< \epsilon_{1f}(\bar{r})\epsilon_{1f}^*(\bar{r}') >= \epsilon_{1m}'^2 \delta \exp[-\frac{(x-x')^2+(y-y')^2}{l_p^2} - \frac{|z-z'|}{l_z}]$$

$z = -d$

Region 2 $\qquad \epsilon_2$

Figure 5.3.1 Geometrical configuration of the problem.

$$\bar{I}_{os}(\theta_{os}, \phi_{os})$$

$$= \int_0^{2\pi} d\phi_o' \int_0^{\pi/2} d\theta_o' \sin \theta_o' \, \overline{\overline{R}}_{01}(\theta_{os}, \phi_{os}; \theta_o', \phi_o') \cdot \bar{I}_{oi}(\pi - \theta_o', \phi_o')$$

$$+ \int_0^{2\pi} d\phi' \int_0^{\pi/2} d\theta' \sin \theta' \, \overline{\overline{T}}_{10}(\theta_{os}, \phi_{os}; \theta', \phi') \cdot \bar{I}(\theta', \phi', z = 0) \quad (67)$$

where $\overline{\overline{T}}_{10}(\theta_o, \phi_o; \theta', \phi')$ represents coupling from region 1 to region 0. The coupling coefficients used in the boundary conditions for the rough interfaces are derived in the next section.

b. Boundary Conditions

The boundary conditions satisfied by the specific intensities at rough dielectric interfaces are derived in this section. Unlike the planar interface case where the coupling at the boundary is only to the specular reflection and transmission directions, the incident intensity is coupled to all of the reflection and transmission directions. The reflection and transmission matrices are related to the bistatic scattering matrices, which is the generalization of the bistatic scattering coefficients to include the correlation between polarizations of the scattered fields.

Consider a plane wave incident from medium 1 onto medium 2 along the direction $\hat{k}_i$ upon a rough dielectric interface. The electric field of the incident wave is given by

$$\overline{E}_i = \hat{e}_i \, E_{ei} \, e^{i\overline{k}_i \cdot \overline{r}} \tag{68}$$

where $\overline{k}_i$ denotes the incident wave vector and $\hat{e}_i$ is the polarization of the electric field vector. The rough surface is characterized by a random height distribution $z = f(\overline{r}_\perp)$ where $f(\overline{r}_\perp)$ is a Gaussian random variable with zero mean, $\langle f(\overline{r}_\perp) \rangle = 0$. The incident field will generate the reflected and transmitted fields in medium 1 and 2, respectively. The solutions to the problem of scattering from a random rough surface have been extensively studied [55-67]. In general, the scattered and transmitted fields for vertical and horizontal polarizations for the incident field with vertical and horizontal polarizations are given by

$$\begin{bmatrix} E_{vs} \\ E_{hs} \end{bmatrix} = \frac{e^{ik_1 r}}{r} \begin{bmatrix} f_{vv}^r(\theta_s, \phi_s; \theta_i, \phi_i) & f_{vh}^r(\theta_s, \phi_s; \theta_i, \phi_i) \\ f_{hv}^r(\theta_s, \phi_s; \theta_i, \phi_i) & f_{hh}^r(\theta_s, \phi_s; \theta_i, \phi_i) \end{bmatrix} \cdot \begin{bmatrix} E_{vi} \\ E_{hi} \end{bmatrix} \tag{69}$$

$$\begin{bmatrix} E_{vt} \\ E_{ht} \end{bmatrix} = \frac{e^{ik_2 r}}{r} \begin{bmatrix} f_{vv}^t(\theta_t, \phi_t; \theta_i, \phi_i) & f_{vh}^t(\theta_t, \phi_t; \theta_i, \phi_i) \\ f_{hv}^t(\theta_t, \phi_t; \theta_i, \phi_i) & f_{hh}^t(\theta_t, \phi_t; \theta_i, \phi_i) \end{bmatrix} \cdot \begin{bmatrix} E_{vi} \\ E_{hi} \end{bmatrix} \tag{70}$$

Now the scattered specific intensities can be expressed in terms of the incident specific intensities.

$$\overline{I}_r = \overline{\overline{R}}_{12} \cdot \overline{I}_i \tag{71}$$

$$\overline{I}_t = \overline{\overline{T}}_{12} \cdot \overline{I}_i \tag{72}$$

where $\bar{I}_i$, $\bar{I}_s$, and $\bar{I}_t$ are the column matrices for the specific intensities containing the four Stokes parameters

$$\bar{I}_\alpha = \begin{bmatrix} I_{v\alpha} \\ I_{h\alpha} \\ U_\alpha \\ V_\alpha \end{bmatrix} \qquad \alpha = i, r, t \tag{73}$$

and

$$\bar{\bar{R}}_{12}(\theta_s, \phi_s; \theta_i, \phi_i) = \frac{1}{A_o \cos\theta_s} \bar{\bar{L}}^r \tag{74}$$

$$\bar{\bar{T}}_{12}(\theta_t, \phi_t; \theta_i, \phi_i) = \frac{1}{A_o \cos\theta_t} \frac{\eta_1}{\eta_2} \bar{\bar{L}}^t \tag{75}$$

with

$$\bar{\bar{L}}^\alpha = \begin{bmatrix} \langle |f^\alpha_{vv}|^2 \rangle & \langle |f^\alpha_{vh}|^2 \rangle & Re\langle (f^{\alpha*}_{vh} f^\alpha_{vv}) \rangle & -Im\langle (f^{\alpha*}_{vh} f^\alpha_{vv}) \rangle \\ \langle |f^\alpha_{hv}|^2 \rangle & \langle |f^\alpha_{hh}|^2 \rangle & Re\langle (f^{\alpha*}_{hh} f^\alpha_{hv}) \rangle & -Im\langle (f^\alpha_{hv} f^{\alpha*}_{hh}) \rangle \\ 2Re\langle (f^\alpha_{vv} f^{\alpha*}_{hv}) \rangle & 2Re\langle (f^\alpha_{vh} f^{\alpha*}_{hh}) \rangle & Re\langle (f^\alpha_{vv} f^{\alpha*}_{hh} + f^\alpha_{vh} f^{\alpha*}_{hv}) \rangle & -Im\langle (f^\alpha_{vv} f^{\alpha*}_{hh} - f^\alpha_{vh} f^{\alpha*}_{hv}) \rangle \\ 2Im\langle (f^\alpha_{vv} f^{\alpha*}_{hv}) \rangle & 2Im\langle (f^\alpha_{vh} f^{\alpha*}_{hh}) \rangle & Im\langle (f^\alpha_{vv} f^{\alpha*}_{hh} + f^\alpha_{vh} f^{\alpha*}_{hv}) \rangle & Re\langle (f^\alpha_{vv} f^{\alpha*}_{hh} - f^\alpha_{vh} f^{\alpha*}_{hv}) \rangle \end{bmatrix}$$

$$\tag{76}$$

Thus, the boundary conditions for the specific intensities at a rough interface is given by

$$\bar{I}_1(\hat{k}_s) = \int_0^{2\pi} d\phi_i \int_0^{\pi/2} d\theta_i \sin\theta_i \bar{\bar{R}}_{12}(\theta_s, \phi_s; \theta_i, \phi_i) \cdot \bar{I}_1(\hat{k}_i) \tag{77}$$

$$\bar{I}_2(\hat{k}_t) = \int_0^{2\pi} d\phi_i \int_0^{\pi/2} d\theta_i \sin\theta_i \bar{\bar{T}}_{12}(\theta_t, \phi_t; \theta_i, \phi_i) \cdot \bar{I}_1(\hat{k}_i) \tag{78}$$

The reflected and transmitted intensities at the directions $\hat{k}_s$ and $\hat{k}_t$ are given by integration of all the scattered intensities which are coupled to that direction from the incident intensity.

The reflection and transmission coupling matrices can also be related to the rough surface bistatic scattering coefficients. First, the

definition of bistatic scattering coefficients is generalized to include the correlation between polarizations. We define the bistatic scattering matrix $\overline{\overline{\gamma}}$ whose elements are given by

$$\gamma_{\alpha\beta}(\theta_s,\phi_s;\theta_i,\phi_i) = 4\pi\frac{\cos\theta_s \, I_{\alpha s}(\theta_s,\phi_s)}{\cos\theta_i \, I_{\beta i}} \qquad \alpha,\beta = 1,2,3,4 \qquad (79)$$

where

$$\overline{I}_\alpha = \begin{bmatrix} I_{1\alpha} \\ I_{2\alpha} \\ I_{3\alpha} \\ I_{4\alpha} \end{bmatrix} = \begin{bmatrix} I_{v\alpha} \\ I_{h\alpha} \\ U_\alpha \\ V_\alpha \end{bmatrix} \qquad \alpha = i,s \qquad (80)$$

The usual bistatic scattering coefficients are

$$\gamma_{vv} = \gamma_{11} \qquad \gamma_{vh} = \gamma_{12} \qquad \gamma_{hv} = \gamma_{21} \qquad \gamma_{hh} = \gamma_{22} \qquad (81)$$

The reflection coupling matrix is related to the bistatic scattering matrix as follows:

$$\overline{\overline{R}}_{12}(\theta_s,\phi_s;\theta_i,\phi_i) = \frac{1}{4\pi}\frac{\cos\theta_i}{\cos\theta_s}\overline{\overline{\gamma}}(\theta_s,\phi_s;\theta_i,\phi_i) \qquad (82)$$

In a similar manner, the transmission coupling matrix can be related to the bistatic scattering coefficients for the transmitted intensities:

$$\overline{\overline{T}}_{12}(\theta_t,\phi_t;\theta_i,\phi_i) = \frac{1}{4\pi}\frac{\cos\theta_i}{\cos\theta_t}\overline{\overline{\gamma}}^t(\theta_t,\phi_t;\theta_i,\phi_i) \qquad (83)$$

The explicit expressions for the reflection and transmission matrices, obtained using the scattered and transmitted fields derived by a combination of Kirchhoff approximation and geometrical optics approach, are given in Appendix D [31,69]. The other solutions for the scattering from a rough dielectric interface, such as small perturbation method (SPM) [65,66] or modified SPM [67,68], can also be used to derive the coupling matrices to be used with the radiative transfer equations.

Note that, in general, the coupling matrices can be broken up into coherent and incoherent components. The coherent components only couple the incident intensity into the specular reflection and transmission directions while the incoherent components couple to all reflection and transmission directions.

$$\overline{\overline{R}}_{12}(\theta_s,\phi_s;\theta_i,\phi_i) = \overline{\overline{R}}_{12}^c(\theta_s,\phi_s;\theta_i,\phi_i) + \overline{\overline{R}}_{12}^i(\theta_s,\phi_s;\theta_i,\phi_i) \qquad (84)$$

$$\overline{\overline{T}}_{12}(\theta_t, \phi_t; \theta_i, \phi_i) = \overline{\overline{T}}_{12}^c(\theta_t, \phi_t; \theta_i, \phi_i) + \overline{\overline{T}}_{12}^i(\theta_t, \phi_t; \theta_i, \phi_i) \qquad (85)$$

c. Fourier Series Expansion

The radiative transfer equations and the associated boundary conditions can be solved using a numerical approach. We use a Fourier-series expansion in the azimuthal direction to eliminate the ϕ-dependence from the radiative transfer equations and obtain a set of equations without the ϕ-dependence [section 5.2.b] The ϕ-dependence from the boundary conditions can also be eliminated using the Fourier-series expansion. We let

$$\overline{I}_{oi}(\pi - \theta_o, \phi_o) = \overline{I}_{oi}\, \delta(\cos\theta_o - \cos\theta_{oi}) \sum_{m=0}^{\infty} \frac{1}{(\delta_m + 1)\pi} \cos m(\phi_o - \phi_{oi}) \tag{86}$$

and, for $\alpha, \beta = 0, 1, 2$,

$$\overline{\overline{R}}_{\alpha\beta}^c(\theta, \phi; \theta', \phi') = \overline{\overline{R}}_{\alpha\beta}^c(\theta)\, \delta(\cos\theta - \cos\theta') \sum_{m=0}^{\infty} \frac{1}{(1 + \delta_m)\pi} \cos m(\phi - \phi') \tag{87a}$$

$$\overline{\overline{R}}_{\alpha\beta}^i(\theta, \phi; \theta', \phi') = \sum_{m=0}^{\infty} \frac{1}{(1 + \delta_m)\pi} \left[\overline{\overline{R}}_{\alpha\beta}^{mc}(\theta, \theta') \cos m(\phi - \phi') \right.$$
$$\left. + \overline{\overline{R}}_{\alpha\beta}^{ms}(\theta, \theta') \sin m(\phi - \phi') \right] \tag{87b}$$

$$\overline{\overline{T}}_{01}^c(\theta, \phi; \theta_o', \phi_o') = \overline{\overline{T}}_{01}^c(\theta_o)\, \delta(\cos\theta_o - \cos\theta_o') \sum_{m=0}^{\infty} \frac{1}{(1 + \delta_m)\pi} \cos m(\phi_o - \phi_o') \tag{88a}$$

$$\overline{\overline{T}}_{01}^i(\theta, \phi; \theta_o', \phi_o') = \sum_{m=0}^{\infty} \frac{1}{(1 + \delta_m)\pi} \left[\overline{\overline{T}}_{01}^{mc}(\theta, \theta_o') \cos m(\phi_o - \phi_o') \right.$$
$$\left. + \overline{\overline{T}}_{01}^{ms}(\theta, \theta_o') \sin m(\phi_o - \phi_o') \right] \tag{88b}$$

where θ_o and θ are related by the Snell's law.

Substituting (86), (87), and (88) into the boundary conditions (65) and (66) and carrying out the $d\phi'$ and $d\phi'_o$ integrations, we obtain the following set of equations. For $0 < \theta < \pi/2$ and $m = 0, 1, 2, \cdots$

$$\bar{I}^{mc}(\pi - \theta, z = 0)$$

$$= \int_0^{\pi/2} d\theta'_o \sin \theta'_o \left[\bar{\bar{T}}^c_{01}(\theta, \theta'_o) \cdot \bar{I}^{mc}_{oi}(\pi - \theta'_o) \right.$$

$$\left. + \bar{\bar{T}}^{mc}_{01}(\theta, \theta'_o) \cdot \bar{I}^{mc}_{oi}(\pi - \theta'_o) \right]$$

$$+ \int_0^{\pi/2} d\theta' \sin \theta' \, \bar{\bar{R}}^c_{10}(\theta, \theta') \cdot \bar{I}^{mc}(\theta', z = 0)$$

$$+ \int_0^{\pi/2} d\theta' \sin \theta' \left[\bar{\bar{R}}^{mc}_{10}(\theta, \theta') \cdot \bar{I}^{mc}(\theta', z = 0) \right.$$

$$\left. - \bar{\bar{R}}^{ms}_{10}(\theta, \theta') \cdot \bar{I}^{ms}(\theta', z = 0) \right] \tag{89a}$$

$$\bar{I}^{ms}(\pi - \theta, z = 0)$$

$$= \int_0^{\pi/2} d\theta'_o \sin \theta'_o \, \bar{\bar{T}}^{ms}_{01}(\theta, \theta'_o) \cdot \bar{I}^{mc}_{oi}(\pi - \theta'_o)$$

$$+ \int_0^{\pi/2} d\theta' \sin \theta' \, \bar{\bar{R}}^c_{10}(\theta, \theta') \cdot \bar{I}^{ms}(\theta', z = 0)$$

$$+ \int_0^{\pi/2} d\theta' \sin \theta' \left[\bar{\bar{R}}^{ms}_{10}(\theta, \theta') \cdot \bar{I}^{mc}(\theta', z = 0) \right.$$

$$\left. + \bar{\bar{R}}^{mc}_{10}(\theta, \theta') \cdot \bar{I}^{ms}(\theta', z = 0) \right] \tag{89b}$$

$$\bar{I}^{mc}(\theta, z = -d) = \int_0^{\pi/2} d\theta' \sin \theta' \, \bar{\bar{R}}^c_{12}(\theta, \theta') \cdot \bar{I}^{mc}(\pi - \theta', z = -d)$$

$$+ \int_0^{\pi/2} d\theta' \sin \theta' \left[\bar{\bar{R}}^{mc}_{12}(\theta, \theta') \cdot \bar{I}^{mc}(\pi - \theta', z = -d) \right.$$

$$\left. - \bar{\bar{R}}^{ms}_{12}(\theta, \theta') \cdot \bar{I}^{ms}(\pi - \theta', z = -d) \right] \tag{90a}$$

$$\overline{I}^{ms}(\theta, z = -d) = \int_0^{\pi/2} d\theta' \sin\theta' \, \overline{\overline{R}}_{12}^c(\theta,\theta') \cdot \overline{I}^{ms}(\pi - \theta', z = -d)$$

$$+ \int_0^{\pi/2} d\theta' \sin\theta' \left[\overline{\overline{R}}_{12}^{ms}(\theta,\theta') \cdot \overline{I}^{mc}(\pi - \theta', z = -d) \right.$$

$$\left. + \overline{\overline{R}}_{12}^{mc}(\theta,\theta') \cdot \overline{I}^{ms}(\pi - \theta', z = -d) \right] \tag{90b}$$

where

$$\overline{I}_{oi}^{mc}(\pi - \theta_o) = \overline{I}_{oi} \frac{1}{(\delta_m + 1)\pi} \delta(\cos\theta_o - \cos\theta_{oi}) \tag{91}$$

Note that the Fourier-series expanded coupling matrices for azimuthally isotropic rough boundaries do not couple the first two Stokes parameters to the last two Stokes parameters. The coupling matrices can be expanded as follows. For $A = R$ or T, and $\alpha, \beta = 0, 1, 2$,

$$\overline{\overline{A}}_{\alpha\beta}^{mc} = \begin{bmatrix} A_{\alpha\beta_{11}}^{mc} & A_{\alpha\beta_{12}}^{mc} & 0 & 0 \\ A_{\alpha\beta_{21}}^{mc} & A_{\alpha\beta_{22}}^{mc} & 0 & 0 \\ 0 & 0 & A_{\alpha\beta_{33}}^{mc} & A_{\alpha\beta_{34}}^{mc} \\ 0 & 0 & A_{\alpha\beta_{43}}^{mc} & A_{\alpha\beta_{44}}^{mc} \end{bmatrix} \tag{92a}$$

$$\overline{\overline{A}}_{\alpha\beta}^{ms} = \begin{bmatrix} 0 & 0 & A_{\alpha\beta_{13}}^{ms} & A_{\alpha\beta_{14}}^{ms} \\ 0 & 0 & A_{\alpha\beta_{23}}^{ms} & A_{\alpha\beta_{24}}^{ms} \\ A_{\alpha\beta_{31}}^{ms} & A_{\alpha\beta_{32}}^{ms} & 0 & 0 \\ A_{\alpha\beta_{41}}^{ms} & A_{\alpha\beta_{42}}^{ms} & 0 & 0 \end{bmatrix} \tag{92b}$$

Thus, the boundary conditions (89) and (90) can be decoupled by defining

$$\overline{I}^{me}(\theta, z) = \begin{bmatrix} I_v^{mc}(\theta, z) \\ I_h^{mc}(\theta, z) \\ U^{ms}(\theta, z) \\ V^{ms}(\theta, z) \end{bmatrix} \tag{93a}$$

$$\overline{I}^{mo}(\theta, z) = \begin{bmatrix} I_v^{ms}(\theta, z) \\ I_h^{ms}(\theta, z) \\ U^{mc}(\theta, z) \\ V^{mc}(\theta, z) \end{bmatrix} \tag{93b}$$

where superscripts e and o stand for even or odd dependence in the first two Stokes parameters. After carrying out the $d\theta_o$ integration, the decoupled boundary conditions are given by, for $\alpha = e$ or o,

$$\overline{I}^{m\alpha}(\pi - \theta, z = 0)$$

$$= \overline{\overline{T}}^c_{01}(\theta_o) \cdot \overline{I}^{m\alpha}_{oi}(\pi - \theta_o) + \overline{\overline{T}}^{m\alpha}_{01}(\theta, \theta_{oi}) \cdot \overline{I}^{m\alpha}_{oi}$$

$$+ \int_0^{\pi/2} d\theta' \sin \theta' \left[\overline{\overline{R}}^c_{10}(\theta, \theta') + \overline{\overline{R}}^{m\alpha}_{10}(\theta, \theta') \right] \cdot \overline{I}^{m\alpha}(\theta', z = 0) \quad (94a)$$

$$\overline{I}^{m\alpha}(\theta, z = -d)$$

$$= \int_0^{\pi/2} d\theta' \sin \theta' \left[\overline{\overline{R}}^c_{12}(\theta, \theta') + \overline{\overline{R}}^{m\alpha}_{12}(\theta, \theta') \right] \cdot \overline{I}^{m\alpha}(\pi - \theta', z = -d)$$

$$\quad (94b)$$

where, for $A = R$ or T, and $\alpha, \beta = 0, 1, 2$,

$$\overline{\overline{A}}^{me}_{\alpha\beta} = \begin{bmatrix} A^{mc}_{\alpha\beta 11} & A^{mc}_{\alpha\beta 12} & -A^{ms}_{\alpha\beta 13} & -A^{ms}_{\alpha\beta 14} \\ A^{mc}_{\alpha\beta 21} & A^{mc}_{\alpha\beta 22} & -A^{ms}_{\alpha\beta 23} & -A^{ms}_{\alpha\beta 24} \\ A^{ms}_{\alpha\beta 31} & A^{ms}_{\alpha\beta 32} & A^{mc}_{\alpha\beta 33} & A^{mc}_{\alpha\beta 34} \\ A^{ms}_{\alpha\beta 41} & A^{ms}_{\alpha\beta 42} & A^{mc}_{\alpha\beta 43} & A^{mc}_{\alpha\beta 44} \end{bmatrix} \quad (95a)$$

$$\overline{\overline{A}}^{mo}_{\alpha\beta} = \begin{bmatrix} A^{mc}_{\alpha\beta 11} & A^{mc}_{\alpha\beta 12} & A^{ms}_{\alpha\beta 13} & A^{ms}_{\alpha\beta 14} \\ A^{mc}_{\alpha\beta 21} & A^{mc}_{\alpha\beta 22} & A^{ms}_{\alpha\beta 23} & A^{ms}_{\alpha\beta 24} \\ A^{ms}_{\alpha\beta 31} & A^{ms}_{\alpha\beta 32} & A^{mc}_{\alpha\beta 33} & A^{mc}_{\alpha\beta 34} \\ A^{ms}_{\alpha\beta 41} & A^{ms}_{\alpha\beta 42} & A^{mc}_{\alpha\beta 43} & A^{mc}_{\alpha\beta 44} \end{bmatrix}. \quad (95b)$$

and, for $\alpha = e$ or o,

$$\overline{I}^{m\alpha}_{oi}(\pi - \theta_o) = \overline{I}^{m\alpha}_{oi} \frac{1}{(\delta_m + 1)\pi} \delta(\cos \theta_o - \cos \theta_{oi}) \quad (96)$$

with

$$\overline{I}^{me}_{oi} = \begin{bmatrix} I_{vi} \\ I_{hi} \\ 0 \\ 0 \end{bmatrix} \quad (97a)$$

$$\bar{I}_{oi}^{mo} = \begin{bmatrix} 0 \\ 0 \\ U_i \\ V_i \end{bmatrix} \tag{97b}$$

The radiative transfer equations for the even and odd series can be obtained in a similar manner in section 5.2.b. We have, for $\alpha = e$ or o and $m = 0, 1, 2, \cdots$

$$\cos\theta \frac{d}{dz}\bar{I}^{m\alpha}(\theta, z) = -K_a\bar{I}^{m\alpha}(\theta, z) - \bar{\bar{K}}_s(\theta) \cdot \bar{I}^{m\alpha}(\theta, z)$$

$$+ \int_0^\pi d\theta' \sin\theta' \,\bar{\bar{P}}^{m\alpha}(\theta, \theta') \cdot \bar{I}^{m\alpha}(\theta', z) \tag{98}$$

where $\bar{\bar{P}}^{m\alpha}(\theta, \theta')$ is defined in a similar manner to (95) [section 5.2.b].

We define m_{max} and m'_{max} to be the number of harmonics that has to be kept in the expansions of the scattering function matrix and the coupling matrices, respectively, such that

$$\bar{\bar{P}}^{mc}(\theta, \theta') \simeq \bar{\bar{P}}^{ms}(\theta, \theta') \simeq 0 \qquad \text{for} \quad m > m_{max} \tag{99}$$

and

$$\bar{\bar{A}}_{\alpha\beta}^{mc} \simeq \bar{\bar{A}}_{\alpha\beta}^{ms} \simeq 0 \qquad\qquad \text{for} \quad m > m'_{max} \tag{100}$$

Then, for $m > m_{max}$ the radiative transfer equations simplify to

$$\cos\theta \frac{d}{dz}\bar{I}^{m\alpha}(\theta, z) = -K_a\bar{I}^{m\alpha} - \bar{\bar{K}}_s(\theta) \cdot \bar{I}^{m\alpha}(\theta, z) \tag{101}$$

where $\alpha = e$ or o. Similarly, for $m > m'_{max}$ the boundary conditions simplify to

$$\bar{I}^{m\alpha}(\pi - \theta, z = 0) = \bar{\bar{T}}_{01}^c(\theta_o) \cdot \bar{I}_{oi}^{m\alpha}(\pi - \theta_o) + \bar{\bar{R}}_{10}^c(\theta) \cdot \bar{I}^{m\alpha}(\theta, z = 0) \tag{102a}$$

and

$$\bar{I}^{m\alpha}(\theta, z = -d) = \bar{\bar{R}}_{12}^c(\theta) \cdot \bar{I}^{m\alpha}(\pi - \theta, z = -d) \tag{102b}$$

where $d\theta'$ integrations are carried out. Thus, for $m > \max[m_{max}, m'_{max}]$, we can use the simplified radiative transfer equations and the boundary conditions, given by (101) and (102), to obtain the solutions analytically without resorting to the numerical approach.

d. Numerical Solution

The set of decoupled radiative transfer equations without the azimuthal dependence for each harmonic can be solved numerically using the Gaussian quadrature method. The integrals in the radiative transfer equations are replaced by Gaussian quadratures, and the resulting system of first-order differential equations with constant coefficients are solved by obtaining eigenvalues and eigenvectors. The numerical solution for the specific intensity is given by, for each harmonic and for even or odd series,

$$\overline{I}^{+} = (\overline{\overline{E}} + \overline{\overline{Q}}) \cdot \overline{\overline{D}}(z) \cdot \overline{x} + (\overline{\overline{E}} - \overline{\overline{Q}}) \cdot \overline{\overline{U}}(z + d) \cdot \overline{y} \qquad (103a)$$

$$\overline{I}^{-} = (\overline{\overline{E}}' + \overline{\overline{Q}}') \cdot \overline{\overline{D}}(z) \cdot \overline{x} + (\overline{\overline{E}}' - \overline{\overline{Q}}') \cdot \overline{\overline{U}}(z + d) \cdot \overline{y} \qquad (103b)$$

where $\overline{I}^{+}$ and $\overline{I}^{-}$ represent the upward and downward propagating intensities and $\overline{x}$ and $\overline{y}$ are the unknown constants [section 5.2.c].

The boundary conditions, which are to be used to determine the unknown constants $\overline{x}$ and $\overline{y}$, can be obtained by discretizing the boundary conditions given by (94). Following the procedure outlined in the Appendix E, we obtain the following set of equations:

$$\overline{I}^{-}(z = 0) = \overline{\overline{R}}_{10} \cdot \overline{I}^{+}(z = 0) + \overline{\overline{T}}_{01} \cdot \overline{I}_{oi}^{-} \qquad (104a)$$

$$\overline{I}^{+}(z = -d) = \overline{\overline{R}}_{12} \cdot \overline{I}^{-}(z = -d) \qquad (104a)$$

Substituting in the expressions for the upward and downward propagating intensities into the above boundary conditions, we obtain the following set of equations for $\overline{x}$ and $\overline{y}$:

$$\left[(\overline{\overline{E}}' + \overline{\overline{Q}}') - \overline{\overline{R}}_{10} \cdot (\overline{\overline{E}} + \overline{\overline{Q}}) \right] \cdot \overline{x}$$

$$+ \left[(\overline{\overline{E}}' - \overline{\overline{Q}}') - \overline{\overline{R}}_{10} \cdot (\overline{\overline{E}} - \overline{\overline{Q}}) \right] \cdot \overline{\overline{D}}(-d) \cdot \overline{y} = \overline{\overline{T}}_{01} \cdot \overline{I}_{oi}^{-} \quad (105a)$$

$$\left[(\overline{\overline{E}} + \overline{\overline{Q}}) - \overline{\overline{R}}_{12} \cdot (\overline{\overline{E}}' + \overline{\overline{Q}}') \right] \cdot \overline{\overline{D}}(-d) \cdot \overline{x}$$

$$+ \left[(\overline{\overline{E}} - \overline{\overline{Q}}) - \overline{\overline{R}}_{12} \cdot (\overline{\overline{E}}' - \overline{\overline{Q}}') \right] \cdot \overline{y} = 0 \qquad (105b)$$

The above equations can be solved for the constants $\overline{x}$ and $\overline{y}$ for each case when the incident intensity is at one of the quadrature angles.

Once the constants $\bar{x}$ and $\bar{y}$ are determined, the scattered intensities from region 1 to region 0, represented by the first term on the right-hand-side of (67), can be determined. We have

$$\bar{I}_{os} = \bar{\bar{T}}_{10} \cdot \bar{I}^+(z = 0)$$

$$= \bar{\bar{T}}_{10} \cdot \left[(\bar{\bar{E}} + \bar{\bar{Q}}) \cdot \bar{x} + (\bar{\bar{E}} - \bar{\bar{Q}}) \cdot \bar{\bar{D}}(-d) \cdot \bar{y} \right] \qquad (106)$$

Thus, the complete solution can be obtained by solving the radiative transfer equations using the Gaussian quadrature method for each harmonic as outlined above and reintroducing the azimuthal dependence. The total scattered intensities in region 0 are given by

$$\bar{I}_{os}(\phi_o) = \left\{ \bar{\bar{R}}_{01}^c + \bar{\bar{T}}_{10}^c \cdot \left[\bar{\bar{I}} - \bar{\bar{R}}_{10}^c \cdot \bar{\bar{R}}_{12}^c \cdot \exp[-\bar{\bar{\mu}}^{-1} \cdot \bar{\bar{K}}_e d] \right]^{-1} \cdot \bar{\bar{T}}_{01}^c \right\}$$

$$\cdot \bar{I}_{oi} \delta(\phi_o - \phi_{oi})$$

$$+ \sum_{m=0}^{m''_{max}} \left\{ \bar{\bar{R}}_{01}^{mc} \cdot \bar{I}_{oi}^{mc} \cos m(\phi_o - \phi_{oi}) + \bar{\bar{R}}_{01}^{ms} \cdot \bar{I}_{oi}^{mc} \sin m(\phi_o - \phi_{oi}) \right.$$

$$+ \bar{\bar{T}}_{10}^c \cdot \bar{I}^{mc+}(z = 0) \cos m(\phi_o - \phi_{oi})$$

$$+ \bar{\bar{T}}_{10}^c \cdot \bar{I}^{ms+}(z = 0) \sin m(\phi_o - \phi_{oi})$$

$$+ \left[\bar{\bar{T}}_{10}^{mc} \cdot \bar{I}^{mc+}(z = 0) - \bar{\bar{T}}_{10}^{ms} \cdot \bar{I}^{ms-}(z = 0) \right] \cos m(\phi_o - \phi_{oi})$$

$$- \bar{\bar{T}}_{10}^c \cdot \left[\bar{\bar{I}} - \bar{\bar{R}}_{10}^c \cdot \bar{\bar{R}}_{12}^c \cdot \exp[-\bar{\bar{\mu}}^{-1} \cdot \bar{\bar{K}}_e d] \right]^{-1}$$

$$\cdot \bar{\bar{T}}_{01}^c \cdot \bar{I}_{oi}^{mc} \cos m(\phi_o - \phi_{oi})$$

$$+ \left[\bar{\bar{T}}_{10}^{ms} \cdot \bar{I}^{mc+}(z = 0) + \bar{\bar{T}}_{10}^{mc} \cdot \bar{I}^{ms-}(z = 0) \right] \sin m(\phi_o - \phi_{oi}) \right\}$$

$$\tag{107}$$

where $m''_{max} = \max[m_{max}, m'_{max}]$ and for $m > m''_{max}$, we have evaluated the scattered intensities analytically and summed them up. Once the scattered intensities in region 0 are obtained, the bistatic scattering
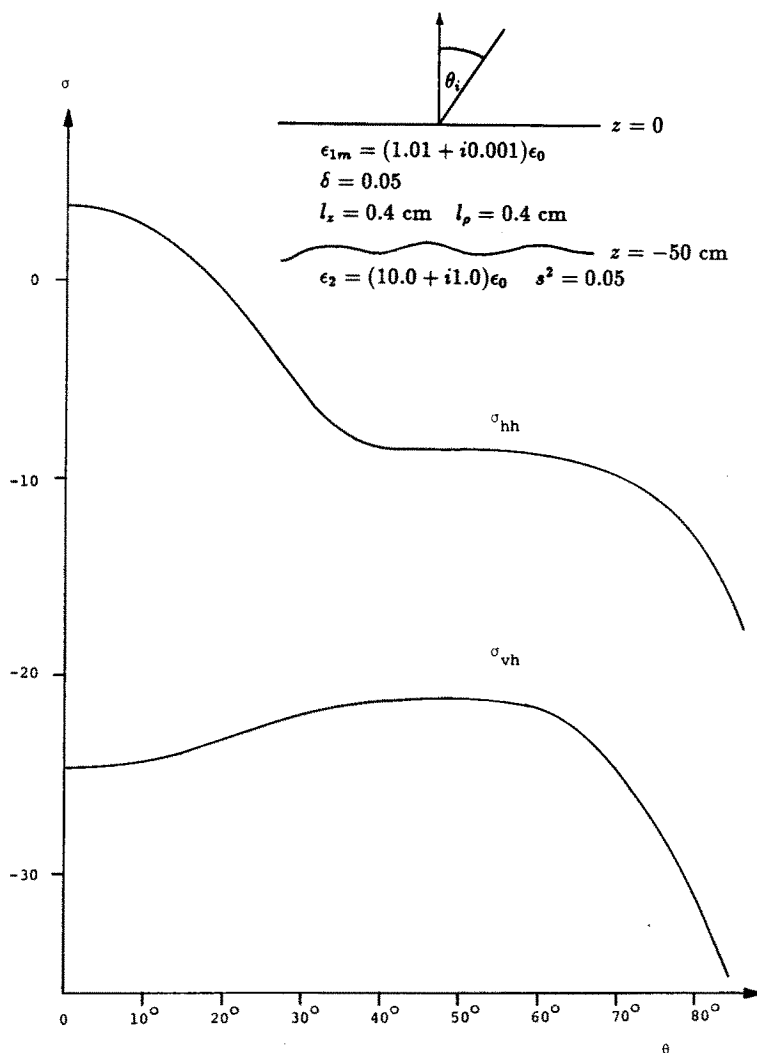
Figure 5.3.2 Backscattering cross sections as a function of incident angle for rough surface and volume scattering at 5 GHz.

coefficients and the backscattering cross sections can be obtained from (7) and (8). It should also be pointed out that the emissivity used in the passive remote sensing, which is related to the bistatic scattering coefficients, can be calculated in a similar manner [70].
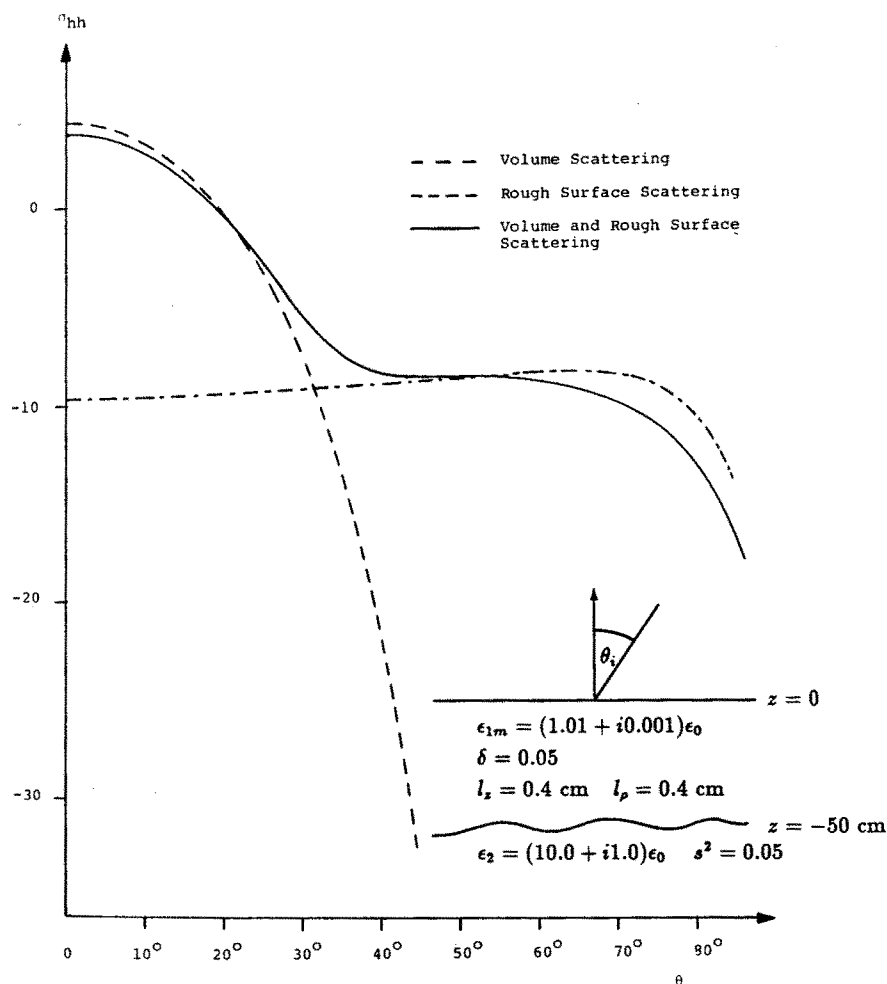
Figure 5.3.3 plot showing backscattering cross sections σ_{hh} versus angle θ

Legend:
- — — Volume Scattering
- - - - - Rough Surface Scattering
- ——— Volume and Rough Surface Scattering

$\epsilon_{1m} = (1.01 + i0.001)\epsilon_0$

$\delta = 0.05$

$l_z = 0.4$ cm $\quad l_\rho = 0.4$ cm

$z = 0$

$z = -50$ cm

$\epsilon_2 = (10.0 + i1.0)\epsilon_0 \quad s^2 = 0.05$

Figure 5.3.3 Backscattering cross sections as a function of incident angle for volume scattering, rough surface scattering, and combined volume and rough surface scattering at 5 GHz.

e. Results and Discussion

In this section we illustrate the theoretical results by plotting backscattering cross sections as functions of incident angle and frequency for various cases. In our calculations $n = 16$ is used. The combined volume and rough surface scattering model is illustrated us-
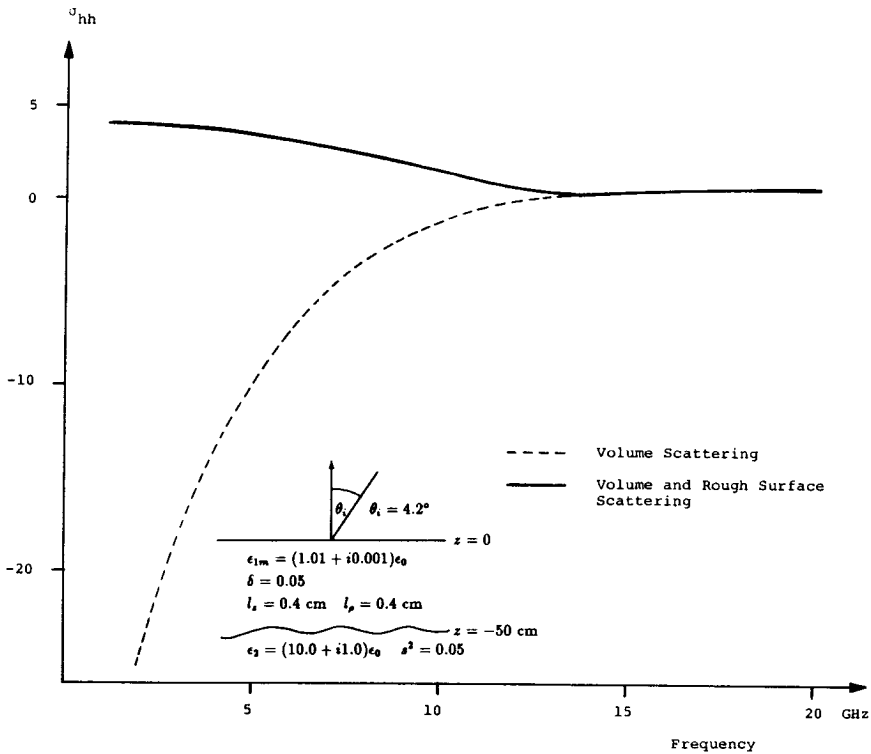
Figure 5.3.4 Backscattering cross sections as a function of frequency for $\theta_i = 4.2°$.

ing the geometrical optics solution for the rough surface modified with the shadowing function. In Fig. 5.3.2, the backscattering cross sections for like-like polarized return σ_{hh} and depolarized return σ_{vh} are plotted as a function of incident angle at 5 GHz. The bottom boundary is assumed to be rough with mean square surface slope $s^2 = 0.05$. We note that unlike the case of only volume scattering, which has a fairly smooth angular dependence, we have a peak near nadir. This is due to the contribution from the bottom rough surface. Also, depolarization return for the combined model is higher than the volume scattering model. In the volume scattering case, the depolarization of the backscattered power is due to the second-order and higher-order scattering effects. However, in the presence of a rough boundary, there
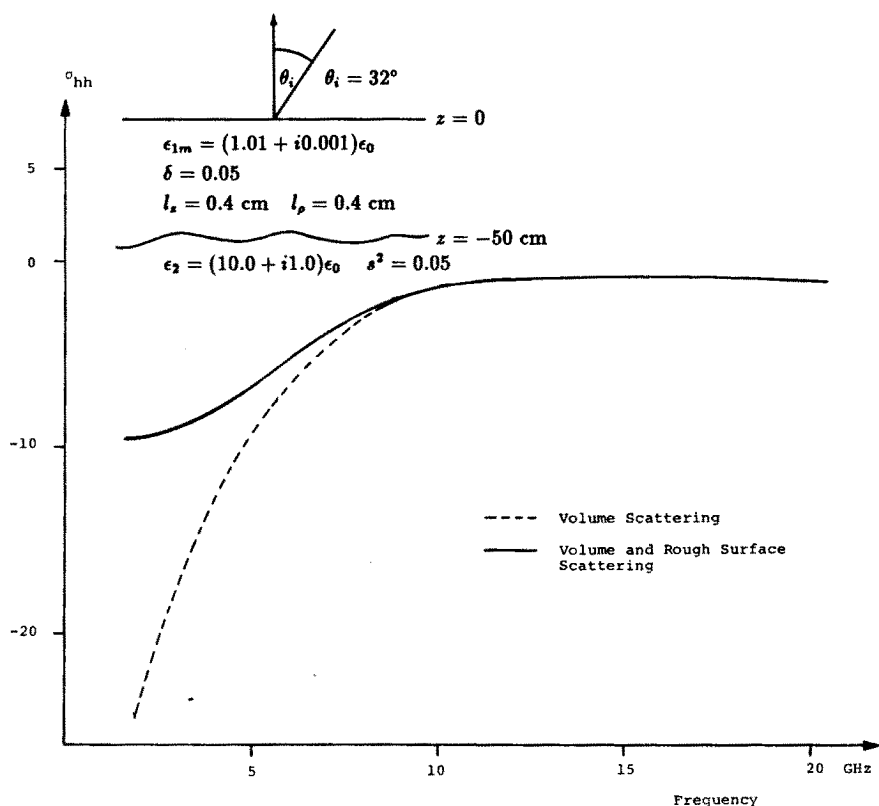
The figure shows a plot with σ_{hh} on the vertical axis and Frequency on the horizontal axis. Axis annotations include:

θ_i, $\theta_i = 32°$

$z = 0$

$\epsilon_{1m} = (1.01 + i0.001)\epsilon_0$

$\delta = 0.05$

$l_z = 0.4$ cm $\quad l_\rho = 0.4$ cm

$z = -50$ cm

$\epsilon_2 = (10.0 + i1.0)\epsilon_0 \quad s^2 = 0.05$

Legend:
- - - - Volume Scattering
—— Volume and Rough Surface Scattering

Vertical axis marks: 5, 0, -10, -20. Horizontal axis marks: 5, 10, 15, 20 GHz. Frequency.

Figure 5.3.5 Backscattering cross sections as a function of frequency for $\theta_i = 32°$.

is the effect of interaction between the rough surface and volume scattering.

In Fig. 5.3.3, we compare the backscattering cross sections for volume scattering, rough surface scattering, and the combined volume and rough surface scattering. We can see that the backscattering cross section near nadir is dominated by the rough surface scattering whereas for larger angles of incidence volume scattering effects dominate.

In Figs. 5.3.4 and 5.3.5, we compare the volume scattering effects and the combined volume and rough surface scattering effects by plotting the backscattering cross sections as a function of frequency. In Fig. 5.3.4 the angle of incidence is $\theta_i = 4.2°$. At low frequencies the backscattered power due to volume scattering diminishes, and the rough surface effects dominate. As frequency is increased the effect of

the bottom rough surface diminishes since the intensities do not penetrate the scattering layer as much as at lower frequencies, and the backscattered power is due to the volume scattering. In Fig. 5.3.5, we illustrate the same case for the angle of incidence $\theta_i = 32°$. Again, the rough surface scattering dominates at low frequencies. However, the rough surface scattering effect diminishes faster as frequency is increased which is due to the fact that at higher incident angles the intensities have to travel a longer path before being affected by the bottom rough surface.

5.4   Summary

In the active microwave remote sensing of earth terrain, scattering effects due to medium inhomogeneities and surface roughness play a dominant role in the determination of radar backscattering coefficients. The volume scattering effects due to medium inhomogeneities have been studied by characterizing earth terrain with two-layer random medium model. The radiative transfer theory is used to calculate the backscattering and bistatic scattering coefficients from a two-layer random medium. Radiative transfer equations are solved numerically using the Fourier series expansion and the Gaussian quadrature method.

In order to more realistically model earth terrain, a composite model comprising an inhomogeneous layer over a homogeneous halfspace with rough boundaries has been developed. The random medium model is used to incorporate the volume scattering effects. To model rough top and bottom interfaces, the bistatic scattering coefficients for a randomly rough surface obtained using a combination of Kirchhoff theory and geometrical optics approach are used. The radiative transfer theory is used to solve for the scattering coefficients. Rough surface effects are incorporated into the radiative transfer theory by modifying the boundary conditions. Radiative transfer equations and the boundary conditions are solved numerically using the Fourier series expansion and the Gaussian quadrature method. It has been shown that the backscattering cross section for the angles of incidence near nadir is dominated by the rough surface effects whereas the large angle of incidence behavior is dominated by the volume scattering effects.

Appendix A: Scattering Function Matrix, Scattering Coefficient, and Absorption Coefficient for the Random Medium

The scattering function matrix has been derived for the random medium whose fluctuating permittivity is characterized by the correlation function

$$\langle \epsilon_f(\overline{r}')\epsilon_f^*(\overline{r}'') \rangle = \delta \epsilon_1'^2 \, b(\overline{r}' - \overline{r}'') \tag{A1}$$

where δ is the variance of the fluctuation, and the function $b(\overline{r}' - \overline{r}'')$ is the normalized correlation function. The scattering function matrix is given by [40]

$$\overline{\overline{P}}(\theta,\phi;\theta',\phi') = \frac{\pi k_1'^4 \delta}{2} \, \Phi(\theta,\phi;\theta',\phi') \begin{bmatrix} p_{11} & p_{12} & p_{13} & 0 \\ p_{21} & p_{22} & p_{23} & 0 \\ p_{31} & p_{32} & p_{33} & 0 \\ 0 & 0 & 0 & p_{44} \end{bmatrix} \tag{A2}$$

where $\Phi(\theta,\phi;\theta',\phi')$ is the spectral density of the fluctuation which is given by the Fourier transform of the correlation function and

$$\begin{aligned} p_{11} &= \sin^2\theta \sin^2\theta' + 2\sin\theta \sin\theta' \cos\theta \cos\theta' \cos(\phi - \phi') \\ &\quad + \cos^2\theta \cos^2\theta' \cos^2(\phi - \phi') \end{aligned} \tag{A3}$$

$$p_{12} = \cos^2\theta \sin^2(\phi - \phi') \tag{A4}$$

$$p_{13} = \cos\theta \sin\theta \sin\theta' \sin(\phi - \phi') + \cos^2\theta \cos\theta' \sin(\phi - \phi')\cos(\phi - \phi') \tag{A5}$$

$$p_{21} = \cos^2\theta' \sin^2(\phi - \phi') \tag{A6}$$

$$p_{22} = \cos^2(\phi - \phi') \tag{A7}$$

$$p_{23} = -\cos\theta' \sin(\phi - \phi')\cos(\phi - \phi') \tag{A8}$$

$$\begin{aligned} p_{31} &= -2\sin\theta \sin\theta' \cos\theta' \sin(\phi - \phi') \\ &\quad - 2\cos\theta \cos^2\theta' \cos(\phi - \phi')\sin(\phi - \phi') \end{aligned} \tag{A9}$$

$$p_{32} = 2\cos\theta \sin(\phi - \phi')\cos(\phi - \phi') \tag{A10}$$

$$p_{33} = \sin\theta \sin\theta' \cos(\phi - \phi') + \cos\theta \cos\theta'[\cos^2(\phi - \phi') - \sin^2(\phi - \phi')] \tag{A11}$$

$$p_{44} = \sin\theta \sin\theta' \cos(\phi - \phi') + \cos\theta \cos\theta' \tag{A12}$$

For the correlation function we assume gaussian dependence laterally and exponential dependence vertically

$$b(\bar{r}' - \bar{r}'') = \exp\left[-\frac{(x'-x'')^2 + (y'-y'')^2}{l_\rho^2} - \frac{|z'-z''|}{l_z}\right] \qquad (A13)$$

Then the spectral density is given by

$$\Phi(\theta, \phi; \theta', \phi') = \frac{l_z l_\rho^2}{4\pi^2[1 + k_1'^2 l_z^2(\cos\theta' - \cos\theta)^2]}$$
$$\cdot \exp\left[-\frac{k_1'^2 l_\rho^2}{4}[\sin^2\theta' + \sin^2\theta - 2\sin\theta'\sin\theta\cos(\phi'-\phi)]\right] \cdot$$
$$(A14)$$

The scattering coefficient $\overline{\overline{K}}_s(\theta)$ is given by

$$\overline{\overline{K}}_s(\theta) = \begin{bmatrix} K_v & 0 & 0 & 0 \\ 0 & K_h & 0 & 0 \\ 0 & 0 & \frac{K_v+K_h}{2} & 0 \\ 0 & 0 & 0 & \frac{K_v+K_h}{2} \end{bmatrix} \qquad (A15)$$

where

$$K_v(\theta') = \int_{4\pi} d\Omega \, \frac{\pi k_1'^4 \delta}{2} \, \Phi(\theta, \phi; \theta', \phi')[p_{11}(\theta, \phi; \theta', \phi') + p_{21}(\theta, \phi; \theta', \phi')]$$
$$(A16)$$

$$K_h(\theta') = \int_{4\pi} d\Omega \, \frac{\pi k_1'^4 \delta}{2} \, \Phi(\theta, \phi; \theta', \phi')[p_{12}(\theta, \phi; \theta', \phi') + p_{22}(\theta, \phi; \theta', \phi')]$$
$$(A17)$$

and the $d\Omega$ integration is carried over a 4π solid angle. The absorption coefficient K_a is given by

$$K_a = 2k_1'' \qquad (A18)$$

where k_1'' is the imaginary part of the wave number in region 1.

Appendix B: Coupling Matrices for Stokes Parameters at Planar Dielectric Interface

The coupling matrices in the boundary conditions take the form [40,53], for $\alpha, \beta = 0, 1, 2$,

$$\overline{\overline{T}}_{\alpha\beta}(\theta_\alpha) = \frac{\epsilon'_\beta}{\epsilon'_\alpha} \begin{bmatrix} t_{v\alpha\beta}(\theta_\alpha) & 0 & 0 & 0 \\ 0 & t_{h\alpha\beta}(\theta_\alpha) & 0 & 0 \\ 0 & 0 & g_{\alpha\beta}(\theta_\alpha) & -h_{\alpha\beta}(\theta_\alpha) \\ 0 & 0 & h_{\alpha\beta}(\theta_\alpha) & g_{\alpha\beta}(\theta_\alpha) \end{bmatrix} \quad (B1)$$

and

$$\overline{\overline{R}}_{\alpha\beta}(\theta_\alpha) = \begin{bmatrix} r_{v\alpha\beta}(\theta_\alpha) & 0 & 0 & 0 \\ 0 & r_{h\alpha\beta}(\theta_\alpha) & 0 & 0 \\ 0 & 0 & W_{\alpha\beta}(\theta_\alpha) & -Z_{\alpha\beta}(\theta_\alpha) \\ 0 & 0 & Z_{\alpha\beta}(\theta_\alpha) & W_{\alpha\beta}(\theta_\alpha) \end{bmatrix} \quad (B2)$$

where

$$t_{v\alpha\beta}(\theta_\alpha) = 1 - r_{v\alpha\beta}(\theta_\alpha) \quad (B3)$$

$$t_{h\alpha\beta}(\theta_\alpha) = 1 - r_{h\alpha\beta}(\theta_\alpha) \quad (B4)$$

$$g_{\alpha\beta}(\theta_\alpha) = (\cos\theta_\beta / \cos\theta_\alpha) Re(Y_{\alpha\beta} X^*_{\alpha\beta}) \quad (B5)$$

$$h_{\alpha\beta}(\theta_\alpha) = (\cos\theta_\beta / \cos\theta_\alpha) Im(Y_{\alpha\beta} X^*_{\alpha\beta}) \quad (B6)$$

for θ_α less than the critical angle, otherwise

$$g_{\alpha\beta}(\theta_\alpha) = h_{\alpha\beta}(\theta_\alpha) = 0 \quad (B7)$$

and

$$X_{\alpha\beta}(\theta_\alpha) = 1 + R_{\alpha\beta}(\theta_\alpha) \quad (B8)$$

$$Y_{\alpha\beta}(\theta_\alpha) = 1 + S_{\alpha\beta}(\theta_\alpha) \quad (B9)$$

where $R_{\alpha\beta}(\theta_\alpha)$ and $S_{\alpha\beta}(\theta_\alpha)$ are the TE and TM Fresnel reflection coefficients, and

$$r_{v\alpha\beta}(\theta_\alpha) = |S_{\alpha\beta}(\theta_\alpha)|^2 \quad (B10)$$

$$r_{h\alpha\beta}(\theta_\alpha) = |R_{\alpha\beta}(\theta_\alpha)|^2 \quad (B11)$$

$$W_{\alpha\beta}(\theta_\alpha) = Re(S_{\alpha\beta} R^*_{\alpha\beta}) \quad (B12)$$

$$Z_{\alpha\beta}(\theta_\alpha) = Im(S_{\alpha\beta} R^*_{\alpha\beta}) \quad (B13)$$

Appendix C: Fourier Series Expansion of the Scattering Function Matrix

The scattering function matrix given in Appendix A can be expanded into the cosine and sine series as follows:

$$\overline{\overline{P}}(\theta, \phi : \theta'\phi') = \sum_{m=0}^{\infty} \frac{1}{(\delta_m + 1)\pi} \left[\overline{\overline{P}}^{mc}(\theta, \theta') \cos m(\phi - \phi') \right.$$
$$\left. + \overline{\overline{P}}^{ms}(\theta, \theta') \sin m(\phi - \phi') \right] \qquad (C1)$$

where

$$\overline{\overline{P}}^{mc}(\theta, \theta') = q(\theta, \theta') \begin{bmatrix} p_{11}^{mc} & p_{12}^{mc} & 0 & 0 \\ p_{21}^{mc} & p_{22}^{mc} & 0 & 0 \\ 0 & 0 & p_{33}^{mc} & p_{34}^{mc} \\ 0 & 0 & p_{43}^{mc} & p_{44}^{mc} \end{bmatrix} \qquad (C2)$$

$$\overline{\overline{P}}^{ms}(\theta, \theta') = q(\theta, \theta') \begin{bmatrix} 0 & 0 & p_{13}^{ms} & p_{14}^{ms} \\ 0 & 0 & p_{23}^{ms} & p_{24}^{ms} \\ p_{31}^{ms} & p_{32}^{ms} & 0 & 0 \\ p_{41}^{ms} & p_{42}^{ms} & 0 & 0 \end{bmatrix} \qquad (C3)$$

with

$$q(\theta, \theta') = \frac{\delta k_1'^4}{4} \frac{l_\rho^2 l_z}{1 + k_1'^2 l_z^2 (\cos \theta - \cos \theta')^2} \qquad (C4)$$

$$p_{11}^{mc} = e^{-y} \left[\sin^2 \theta \sin^2 \theta' I_m(x) + \sin \theta \sin \theta' \cos \theta \cos \theta' (I_{m-1}(x) + I_{m+1}(x)) \right.$$
$$\left. + \cos^2 \theta \cos^2 \theta' (\frac{1}{2} I_m(x) + \frac{1}{4} I_{m-2}(x) + \frac{1}{4} I_{m+2}(x)) \right] \qquad (C5)$$

$$p_{12}^{mc} = e^{-y} \cos^2 \theta \frac{1}{2} \left[I_m(x) - \frac{1}{2}(I_{m-2}(x) + I_{m+2}(x)) \right] \qquad (C6)$$

$$p_{21}^{mc} = e^{-y} \cos^2 \theta' \frac{1}{2} \left[I_m(x) - \frac{1}{2}(I_{m-2}(x) + I_{m+2}(x)) \right] \qquad (C7)$$

$$p_{22}^{mc} = e^{-y} \frac{1}{2} \left[I_m(x) + \frac{1}{2}(I_{m-2}(x) + I_{m+2}(x)) \right] \qquad (C8)$$

$$p_{33}^{mc} = e^{-y}\frac{1}{2}\Big[\sin\theta\sin\theta'(I_{m-1}(x) + I_{m+1}(x))$$

$$+ \cos\theta\cos\theta'(I_{m-2}(x) + I_{m+2}(x))\Big] \qquad (C9)$$

$$p_{44}^{mc} = e^{-y}\Big[\cos\theta\cos\theta' I_m(x) + \sin\theta\sin\theta'\frac{1}{2}(I_{m-1}(x) + I_{m+1}(x))\Big]$$

$$(C10)$$

$$p_{34}^{mc} = p_{43}^{mc} = 0 \qquad (C11)$$

$$p_{13}^{ms} = e^{-y}\cos\theta\frac{1}{2}\Big[\sin\theta\sin\theta'(I_{m-1}(x) - I_{m+1}(x))$$

$$+ \frac{1}{2}\cos\theta\cos\theta'(I_{m-2}(x) - I_{m+2}(x))\Big] \qquad (C12)$$

$$p_{23}^{ms} = -e^{-y}\cos\theta'\frac{1}{4}(I_{m-2}(x) - I_{m+2}(x)) \qquad (C13)$$

$$p_{31}^{ms} = -e^{-y}\cos\theta'\Big[\sin\theta\sin\theta'(I_{m-1}(x) - I_{m+1}(x))$$

$$+ \frac{1}{2}\cos\theta\cos\theta'(I_{m-2}(x) - I_{m+2}(x))\Big] \qquad (C14)$$

$$p_{32}^{ms} = e^{-y}\cos\theta\frac{1}{2}(I_{m-2}(x) - I_{m+2}(x)) \qquad (C15)$$

$$p_{14}^{ms} = p_{24}^{ms} = p_{41}^{ms} = p_{42}^{ms} = 0 \qquad (C16)$$

$$y = \frac{1}{4}k_1'^2 l_\rho^2(\sin^2\theta + \sin^2\theta') \qquad (C17)$$

$$x = \frac{1}{2}k_1'^2 l_\rho^2\sin\theta\sin\theta' \qquad (C18)$$

and I_m is the m-th order modified Bessel function.

Appendix D: Expressions for Coupling Matrices Obtained using Geometrical Optics Solution

The reflection and transmission coupling matrices at the rough dielectric interface can be obtained using the scattered and the transmitted fields derived by a combination of Kirchhoff approximation and

geometrical optics approach. The explicit expressions for the coupling matrices $\overline{\overline{R}}_{12}$ and $\overline{\overline{T}}_{12}$ are given by [31]

$$\overline{\overline{R}}_{12}(\theta_s, \phi_s; \theta_i, \phi_i) = \frac{1}{\cos\theta_s} \frac{|\overline{k}_{1d}|^4}{4|\hat{k}_i \times \hat{k}_s|^4 k_{1dz}^4} \frac{1}{2\pi s^2}$$
$$\cdot \exp\left[-\frac{k_{1dx}^2 + k_{1dy}^2}{2k_{1dz}^2 s^2}\right] \overline{\overline{C}}_{12}^{R}(\theta_s, \phi_s; \theta_i, \phi_i) \quad (D1)$$

$$\overline{\overline{T}}_{12}(\theta_t, \phi_t; \theta_i, \phi_i) = \frac{1}{\cos\theta_t} \frac{k_2^2 |\overline{k}_{2d}|^2 (\hat{n}\cdot\hat{k}_t)^2}{|\hat{k}_i \times \hat{k}_t|^4 k_{2dz}^4} \frac{\eta_1}{\eta_2} \frac{1}{2\pi s^2}$$
$$\cdot \exp\left[-\frac{k_{2dx}^2 + k_{2dy}^2}{2k_{2dz}^2 s^2}\right] \overline{\overline{C}}_{12}^{T}(\theta_t, \phi_t; \theta_i, \phi_i) \quad (D2)$$

where s^2 is the mean square surface slope

$$\overline{k}_{1d} = \overline{k}_i - \overline{k}_s \quad (D3)$$

$$\overline{k}_{2d} = \overline{k}_i - \overline{k}_t \quad (D4)$$

$$\overline{\overline{C}}_{12}^{\alpha} = \begin{bmatrix} |f_{vv}^{\alpha}|^2 & |f_{vh}^{\alpha}|^2 & Re(f_{vh}^{\alpha*}f_{vv}^{\alpha}) & -Im(f_{vh}^{\alpha*}f_{vv}^{\alpha}) \\ |f_{hv}^{\alpha}|^2 & |f_{hh}^{\alpha}|^2 & Re(f_{hh}^{\alpha*}f_{hv}^{\alpha}) & -Im(f_{hv}^{\alpha*}f_{hh}^{\alpha*}) \\ 2Re(f_{vv}^{\alpha}f_{hv}^{\alpha*}) & 2Re(f_{vh}^{\alpha}f_{hh}^{\alpha*}) & Re(f_{vv}^{\alpha}f_{hh}^{\alpha*}+f_{vh}^{\alpha}f_{hv}^{\alpha*}) & -Im(f_{vv}^{\alpha}f_{hh}^{\alpha*}-f_{vh}^{\alpha}f_{hv}^{\alpha*}) \\ 2Im(f_{vv}^{\alpha}f_{hv}^{\alpha*}) & 2Im(f_{vh}^{\alpha}f_{hh}^{\alpha*}) & Im(f_{vv}^{\alpha}f_{hh}^{\alpha*}+f_{vh}^{\alpha}f_{hv}^{\alpha*}) & Re(f_{vv}^{\alpha}f_{hh}^{\alpha*}-f_{vh}^{\alpha}f_{hv}^{\alpha*}) \end{bmatrix}$$

$$(D5)$$

with
$$f_{vv}^{r} = (\hat{h}_s \cdot \hat{k}_i)(\hat{h}_i \cdot \hat{k}_s)R_h + (\hat{v}_s \cdot \hat{k}_i)(\hat{v}_i \cdot \hat{k}_s)R_v \quad (D6)$$

$$f_{hv}^{r} = -(\hat{v}_s \cdot \hat{k}_i)(\hat{h}_i \cdot \hat{k}_s)R_h + (\hat{h}_s \cdot \hat{k}_i)(\hat{v}_i \cdot \hat{k}_s)R_v \quad (D7)$$

$$f_{vh}^{r} = (\hat{h}_s \cdot \hat{k}_i)(\hat{v}_i \cdot \hat{k}_s)R_h - (\hat{v}_s \cdot \hat{k}_i)(\hat{h}_i \cdot \hat{k}_s)R_v \quad (D8)$$

$$f_{hh}^{r} = (-\hat{v}_s \cdot \hat{k}_i)(\hat{v}_i \cdot \hat{k}_s)R_h + (\hat{h}_s \cdot \hat{k}_i)(\hat{h}_i \cdot \hat{k}_s)R_v \quad (D9)$$

and
$$f_{vv}^{t} = (\hat{h}_t \cdot \hat{k}_i)(\hat{h}_i \cdot \hat{k}_t)(1 + R_h') + (\hat{v}_t \cdot \hat{k}_i)(\hat{v}_i \cdot \hat{k}_t)\frac{\eta_2}{\eta_1}(1 + R_v') \quad (D10)$$

$$f_{hv}^t = -(\hat{v}_t \cdot \hat{k}_i)(\hat{h}_i \cdot \hat{k}_t)(1 + R_h') + (\hat{h}_t \cdot \hat{k}_i)(\hat{v}_i \cdot \hat{k}_t)\frac{\eta_2}{\eta_1}(1 + R_v') \quad (D11)$$

$$f_{vh}^t = -(\hat{h}_t \cdot \hat{k}_i)(\hat{v}_i \cdot \hat{k}_t)(1 + R_h') + (\hat{v}_t \cdot \hat{k}_i)(\hat{h}_i \cdot \hat{k}_t)\frac{\eta_2}{\eta_1}(1 + R_v') \quad (D12)$$

$$f_{hh}^t = (\hat{v}_t \cdot \hat{k}_i)(\hat{v}_i \cdot \hat{k}_t)(1 + R_h') + (\hat{h}_t \cdot \hat{k}_i)(\hat{h}_i \cdot \hat{k}_t)\frac{\eta_2}{\eta_1}(1 + R_v') \quad (D13)$$

R_v and R_h and R_v' and R_h' are the local reflection coefficients for the vertical and horizontal polarizations evaluated at the stationary phase points (α_o, β_o) and (α_o', β_o'), respectively.

The geometrical optics solution used to derive the boundary conditons for rough dielectric interface satisfies the principle of reciprocity but violates the principle of energy conservation. This is due to the neglect of the effects of multiple scattering and shadowing. The shadowing effects can be incorporated to modify the boundary conditions as follows

$$\overline{\overline{R}}_{12}^m(\hat{k}_s; \hat{k}_i) = S(\hat{k}_s, \hat{k}_i)\overline{\overline{R}}_{12}(\hat{k}_s; \hat{k}_i) \quad (D14)$$

$$\overline{\overline{T}}_{12}^m(\hat{k}_t; \hat{k}_i) = S(\hat{k}_t, \hat{k}_i)\overline{\overline{T}}_{12}(\hat{k}_t; \hat{k}_i) \quad (D15)$$

where $S(\hat{k}_\alpha, \hat{k}_\beta)$ is the probability that a point will be illuminated by rays having the directions $\hat{k}_\beta$ and $-\hat{k}_\alpha$, given the values of the slope at the point [31].

Appendix E: Application of Legendre Quadrature Formula to the Boundary Conditions

The boundary conditions given by (94) can be cast into the matrix form using the quadrature formula. In this appendix we will illustrate the application of the Legendre quadrature formula to the boundary conditions. The boundary conditions are approximated in a manner such that the formulation does not have to be changed when applied to the flat surface case.

Consider the following scalar version of the boundary condition at $z = -d$:

$$I(\theta, z = -d) = \int_0^{\pi/2} d\theta' \sin\theta' \, r_{12}(\theta, \theta') I(\pi - \theta', z = -d) \quad (E1)$$

One way to approximate the above equations is to apply the Gaussian quadrature method. We obtain, for $i, j = 1, 2, \cdots, n$,

$$I(\theta_i, z = -d) = \sum_{j=1}^n a_j \, r_{12}(\theta_i, \theta_j) I(\pi - \theta_j, z = -d) \quad (E2)$$

This approach is justified as long as the approximation of changing the integration to the summation is accurate. This means the number of quadrature points n has to be large enough so that the above approximation is valid. Note that as $r_{12}(\theta, \theta')$ becomes a more sharply peaked function at the specular direction, the number of quadrature points has to be increased. Thus, it would be difficult to use the above approach for the case of near specular surface. In the limit of specular surface the coupling function is given by

$$r_{12}(\theta, \theta') = r_{12}(\theta)\, \delta(\cos\theta' - \cos\theta) \qquad (E3)$$

and the boundary condition simplifies to

$$I(\theta, z = -d) = r_{12}(\theta)I(\pi - \theta, z = -d) \qquad (E4)$$

In this limit we note that the number of quadrature points does not have to be large as long as $r_{12}(\theta)$ is a fairly smooth function.

One way to overcome the above problem is to use the Legendre quadrature formula. We let $\mu = \cos\theta$. Then, for $i = 1, 2, \cdots, n$ and $j = -n, \cdots, -1, 1, 2, \cdots, n$,

$$I(\mu_i, z = -d) = \sum_{j=-n}^{n} w_{ij}\, I(\mu_j, z = -d) \qquad (E5)$$

where

$$w_{ij} = \frac{1}{\Pi'(\mu_j)} \int_0^1 d\mu\, r_{12}(\mu_i, \mu)\frac{\Pi(\mu)}{\mu - \mu_j} \qquad (E6)$$

$$\Pi(\mu) = (\mu - \mu_1)(\mu - \mu_2)\cdots(\mu - \mu_n)(\mu + \mu_1)(\mu + \mu_2)\cdots(\mu + \mu_n) \qquad (E7)$$

$$\Pi'(\mu_j) = \frac{d}{d\mu}\Pi(\mu)\bigg|_{\mu=\mu_j} \qquad (E8)$$

$$\mu_j = \cos\theta_j \qquad\qquad \mu_{-j} = \cos(\pi - \theta_j) \qquad (E9)$$

In the above formulation, we note that as $r_{12}(\mu, \mu')$ becomes a sharply peaked function around the specular direction, the number of quadrature angles n does not have to be increased as long as the coefficients w_{ij} are evaluated accurately. In the limit of specular surface, we have

$$w_{ij} = r_{12}(\mu_j)\, \delta_{ij} \qquad (E10)$$

where

$$\delta_{ij} = \begin{cases} 1 & \text{if } i = j \\ 0 & \text{otherwise} \end{cases} \qquad (E11)$$

Therefore, in the limit of specular surface, we have

$$I(\theta_i, z = -d) = r_{12}(\theta_i)I(\pi - \theta_i, z = -d) \qquad (E12)$$

Thus, if we use the Legendre quadrature formula to discretize the boundary conditions, then as the surface becomes more specular the number of quadrature angles does not have to be increased, and also the formulation does not have to be changed.

The boundary condition $(E5)$ can be cast into the following matrix equation:

$$\overline{I}^+(z = -d) = \overline{\overline{W}}_{12} \cdot \overline{I}^-(z = -d) + \overline{\overline{U}}_{12} \cdot \overline{I}^+(z = -d) \qquad (E13)$$

where

$$\overline{I}^+(z = -d) = \begin{bmatrix} I(\mu_1, z = -d) \\ \vdots \\ I(\mu_n, z = -d) \end{bmatrix} \qquad \overline{I}^-(z = -d) = \begin{bmatrix} I(\mu_{-1}, z = -d) \\ \vdots \\ I(\mu_{-n}, z = -d) \end{bmatrix} \qquad (E14)$$

$$\overline{\overline{W}}_{12} = \begin{bmatrix} w_{11} & \cdots & w_{1n} \\ \vdots & \vdots & \vdots \\ w_{n1} & \cdots & w_{nn} \end{bmatrix} \qquad (E15)$$

$$\overline{\overline{U}}_{12} = \begin{bmatrix} w_{1(-1)} & \cdots & w_{1(-n)} \\ \vdots & \vdots & \vdots \\ w_{n(-1)} & \cdots & w_{n(-n)} \end{bmatrix} \qquad (E16)$$

Thus, the appropriate boundary condition is given by

$$\overline{I}^+(z = -d) = \overline{\overline{R}}_{12} \cdot \overline{I}^-(z = -d) \qquad (E17)$$

where

$$\overline{\overline{R}}_{12} = [\overline{\overline{I}} - \overline{\overline{U}}_{12}]^{-1} \cdot \overline{\overline{W}}_{12} \qquad (E18)$$

We note that

$$\overline{\overline{U}}_{12} \simeq 0 \qquad (E19)$$

and the coupling matrix is given by

$$\overline{\overline{R}}_{12} = \overline{\overline{W}}_{12} \qquad (E20)$$

The boundary condition at $z = 0$ is next considered. Unlike the boundary condition at $z = -d$, there is an additional source term, which is the incident intensity being transmitted from the upper region. Consider the following scalar version of the boundary condition at $z = 0$:

$$I(\pi - \theta, z = 0) = g(\theta, \theta_{oi}) + \int_0^{\pi/2} d\theta' \sin \theta'\, r_{10}(\theta, \theta')\, I(\theta', z = 0) \quad (E21)$$

where $g(\theta, \theta_{oi})$ represents the incident intensity at θ_{oi} transmitted from region 0 to region 1. The second term in the left-side of the above equation can be approximated following the same procedure outlined above for the boundary condition at $z = -d$. Thus, we will concentrate on approximating the source term $g(\theta, \theta_{oi})$.

We note that for $g(\theta, \theta_{oi})$ which is a smooth function, there is no problem as long as the number of quadrature angles is sufficiently large. Then, the boundary condition can be discretized in a straight-forward manner. In the limit of a specular surface, the source term is given by the delta function, and another approach must be used. One way to bypass the problem of discretizing the delta function is to change the source term at the boundary into the source term in the volume by calculating the zeroth-order solution explicitly and using the radiative transfer equations for the higher order terms with the zeroth-order solution acting as the volume source [51]. However, this approach requires two different formulations for the rough and planar boundaries. Also, the case of near specular surface where the source term is very sharply peaked in the specular direction cannot be treated easily.

In section 5.2, we outlined the procedure for discretizing the delta function and keeping the source term at the boundary. This approach also gives the same solution as the other approach of using the volume source terms. We will now generalize that procedure and discretize the sharply peaked incident intensity. Consider an integral given by

$$I = \int_0^{\pi/2} f(\theta, \theta')\, g(\theta', \theta_{oi}) \qquad (E22)$$

where $f(\theta, \theta')$ is a smooth function. Using the Gaussian quadrature method, the integral I is approximated as

$$I \simeq \sum_{j=-n}^{j=n} a_j \, f(\theta, \theta_j) \, g_j \qquad (E23)$$

Our task is to come up with a set of coefficients g_j, such that the above approximation is accurate for an arbitrary function $g(\theta', \theta_{oi})$. Using the Legendre quadrature formula, the integral I is accurately approximated as

$$I \simeq \sum_{j=-n}^{j=n} f(\theta, \theta_j) \, w_j \qquad (E24)$$

where

$$w_j = \frac{1}{\Pi'(\mu_j)} \int_{-1}^{1} d\mu \, g(\mu, \mu_{oi}) \frac{\Pi(\mu)}{\mu - \mu_j} \qquad (E25)$$

Comparing $(E23)$ and $(E24)$, we obtain

$$g_j = \frac{1}{a_j} w_j \qquad (E26)$$

If we now let $g(\theta', \theta_{oi}) = \delta(\cos \theta'_o - \cos \theta_{oi})$ where θ_{oi} is one of the quadrature angles in region 0, the coefficient w_j is given by

$$w_j = \delta_{ji} \frac{\epsilon_o}{\epsilon'_1} \frac{\cos \theta_{oi}}{\cos \theta_i} \qquad (E27)$$

Thus, the discrete form for the delta function is given by

$$g_j = \delta_{ji} \frac{1}{a_j} \frac{\epsilon_o}{\epsilon'_1} \frac{\cos \theta_{oi}}{\cos \theta_i} \qquad (E28)$$

which is the same as the result given in Section II.3, Eq. (60). If $g(\theta', \theta_{oi})$ is a smooth function, then the coefficient w_j can be approximated as

$$w_j \simeq g(\mu_j, \mu_{oi}) \frac{1}{\Pi'(\mu_j)} \int_{-1}^{1} d\mu \frac{\Pi(\mu)}{\mu - \mu_j}$$

$$= g(\mu_j, \mu_{oi}) a_j \qquad (E29)$$

Therefore,

$$g_j = g(\mu_j, \mu_{oi}) \qquad (E30)$$

which is also a consistent result. Thus, the discretization of the source term by $(E24)$ and $(E25)$ gives the correct results in both limits of very sharply peaked and smooth incident intensities. We also note that

$$w_j \simeq 0 \qquad \text{for} \quad j = -1, -2, \cdots, -n \qquad (E31)$$

Acknowledgments

References

[1] Rouse, J. W., Jr., "Arctic ice type identification by radar," *Proc. IEEE*, **57**, 605–611, 1969.

[2] Johnson, J. D. and L. D. Farmer, "Use of side-looking airborne radar for sea ice identification," *J. Geophys. Res.*, **76**, 2138–2155, 1971.

[3] Edgerton, A. T., A. Stogryn, and G. Poe, "Microwave radiometric investigations of snowpacks," Final Report 1285R-4, Aerojet-General Corp., El Monte, CA, 1971.

[4] Meier, M. F., "Application of remote sensing techniques to the study of seasonal snow cover," *J. Glaciology*, **15**, 251–265, 1975.

[5] Gloersen, P., W. Nordberg, T. J. Schmugge, T. T. Wilheit, and W. J. Campbell, "Microwave signatures of first-year and multiyear sea ice," *J. Geophys. Res.*, **78**, 3564–3572, 1973.

[6] Ketchum, R. D., Jr. and S. G. Tooma, Jr., "Analysis and interpretation of air-borne multifrequency side-looking radar sea ice imagery," *J. Geophys. Res.*, **3**, 520–538, 1973.

[7] Elachi, C., M. L. Bryaand, and W. F. Weeks, "*Imaging radar observations of frozen Arctic lakes,*" *Rem. Sens. Environ.*, **5**, 169–175, 1976.

[8] Kunzi, K. F., A. D. Fisher, D. H. Staelin, and J. W. Waters, "Snow and ice surfaces measured by the Nimbus-5 microwave spectrometer," *J. Geophys. Res.*, **81**, 4965–4980, 1976.

[9] Parashar, S. K., R. M. Haralick, R. K. Moore, and A. W. Biggs, "Radar scatterometer discrimination of sea-ice types," *IEEE Trans. Geosci. Electron.*, **GE-15**, 83–87, 1977.

[10] Ulaby, F. T., W. H. Stiles, L. F. Dellwig, and B. C. Hanson, "Experiments on the radar backscatter of snow," *IEEE Trans. Geosci. Electron.*, **GE-15**, 185–189, 1977.

[11] Zwally, H. J., "Microwave emissivity and accumulation rate of polar firn," *J. Glaciology*, **18**, 195–215, 1977.

[12] Hofer, R. and E. Schanda, "Signatures of snow in the 5 to 94 GHz range, " *Radio Science*, **13**, 365–369, 1978.

[13] Shiue, J. C., A. T. C. Chang, H. Boyne, and D. Ellerbruch, "Remote sensing of snowpack with microwave radiometers for hydrologic applications," *Proceedings of the 12th International Symposium on Remote Sensing of Environment*, **2**, 877–886, Univ. of Michigan, Ann Arbor, MI, 1978.

[14] Stiles, W. H. and F. T. Ulaby, "The active and passive microwave response to snow parameters: 1. Wetness," *J. Geophys. Res.*, **85**, 1037–1044, 1980.

[15] Rango, A., A. T. C. Chang, and J. L. Foster, "The utilization of spaceborne microwave radiometers for monitoring snowpack properties," *Nordic Hydrol.*, **10**, 25–40, 1979.

[16] Ulaby, F. T., "Radar response to vegetation," *IEEE Trans. Ant. Prop.*, **AP-23**, 36–45, 1975.

[17] Ulaby, F. T., T. F. Bush and P. P. Batlivala, "Radar response to vegetation II: 8-18 GHz band," *IEEE Trans. Ant. Prop.*, **AP-23**, 608–618, 1975.

[18] Bush, T. F. and F. T. Ulaby, "Radar return from a continuous vegetation canopy," *IEEE Trans. Ant. Prop.*, **AP-24**, 269–276, 1976.

[19] Bush, T. F. and F. T. Ulaby, "An evaluation of radar as a crop classifier," *Rem. Sens. Environ.,* **7,** 15–36, 1978.

[20] Grody, N. C., "Remote sensing of atmospheric water content from satellites using microwave radiometry," *IEEE Trans. Ant. Prop.,* **AP-24,** 1976.

[21] Tsang, L., J. A. Kong, E. Njoku, D. H. Staelin, and J. Waters, "Theory for microwave thermal emission from a layer of cloud or rain," *IEEE Trans. Ant. Prop.,* **AP-25,** 650–657, 1977.

[22] Dickey, F. M., C. King, J.C. Holtzman, and R. K. Moore, "Moisture dependency of radar backscatter from irrigated and non-irrigated fields at 400 MHz and 13.3 GHz," *IEEE Trans. Geosci. Electron.,* **GE-12,** 19–22, 1974.

[23] Schmugge, T. J., P. Gloerson, T. Wilheit, and F. Geiger, "Remote sensing of soil moisture with microwave radiometers," *J. Geophys. Res.,* **9,** 317–323, 1974.

[24] Ulaby, F. T. and P. P. Batlivala, "Optimum radar parameters for mapping soil moisture," *IEEE Trans. Geosci. Electron.,* **GE-14,** 81–93, 1976.

[25] Njoku, E. G. and J. A. Kong, "Theory for passive sensing of near-surface soil moisture," *J. Geophys. Res.,* **82,** 3108–3118, 1977.

[26] Newton, R. W. and J. W. Rouse, Jr., "Microwave radiometer measurements of soil moisture constant," *IEEE Trans. Ant. Prop.,* **AP-28,** 680–686, 1980.

[27] Wang, J. R., R. W. Newton, and J. W. Rouse, "Passive microwave remote sensing of soil moisture: The effect of tilled row structure," *IEEE Trans. Geosci. Remote Sens.,* **GE-18,** 296–302, 1980.

[28] Jackson, T. J. and T. J. Schmugge, "Aircraft active microwave measurements for estimating soil moisture," *Photogrammetr. Eng. and Remote Sens.,* **47,** 801–805, 1981.

[29] Njoku, E. G. and P. E. O'Neill, "Multifrequency microwave radiometer measurements of soil moisture," *IEEE Trans. Geosci. Remote Sens.,* **GE-20,** 468–475, 1981.

[30] Wang, J. R., P. E. O'Neill, T. J. Jackson, and E. T. Engman, "Multifrequency measurements of the effects of soil moisture, soil texture and surface roughness," *IEEE Trans. Geosci. Remote Sens.,*

GE-21, 44–51, 1983.

[31] Tsang, L., J. A. Kong, and R. T. Shin, *Theory of Microwave Remote Sensing*, Wiley-Interscience, NY, 1985.

[32] Gurvich, A. S., V. L. Kalinin, and D. T. Matveyer, "Influence of internal structure of glaciers on their thermal radio emission," *Atm. Oceanic Phys.* USSR, **9**, 713–717, 1973.

[33] Tsang, L. and J. A. Kong, "The brightness temperature of a half-space random medium with nonuniform temperature profile," *Radio Science,* **10**, 1025–1033, 1975.

[34] England, A. W., "Thermal microwave emission from a halfpace containing scatterers," *Radio Science,* **9**, 447–454, 1974.

[35] England, A. W., "Thermal microwave emission from a scattering layer," *J. Geophys. Res.,* **80**, 4484–4496, 1975.

[36] Tsang, L. and J. A. Kong, "Emissivity of half-space random media," *Radio Science,* **11**, 593–598, 1976a.

[37] Tsang, L. and J. A. Kong, "Thermal microwave emission from a halfpace random media," *Radio Science,* **11**, 599–610, 1976b.

[38] Stogryn, A., "Electromagnetic scattering by random dielectric constant fluctuations in a bounded medium," *Radio Science,* **9**, 509–518, 1970.

[39] Leader, J. C., "Polarization dependence in EM scattering from Rayleigh scatterers embedded in a dielectric slab. I. Theory," *J. Appl. Phys.,* **46**, 4371–4385, 1975.

[40] Tsang, L. and J. A. Kong, "Radiative transfer theory for active remote sensing of half space random media," *Radio Science,* **13**, 763–774, 1978.

[41] Fung, A. K. and H. S. Fung, "Application of first order renormalization method to scattering from a vegetated-like half space," *IEEE Trans. Geosci. Electron.,* GE-15, 189–195, 1977.

[42] Fung, A. K., "Scattering from a vegetation layer," *IEEE Trans. Geosci. Electron.,* **GE-17**, 1–5, 1979.

[43] Zuniga, M. and J. A. Kong, "Active remote sensing of random media," *J. Appl. Phys.,* **51**, 74–79, 1980.

[44] Zuniga, M., J. A. Kong, and L. Tsang, "Depolarization effects in

the remote sensing of random media," *J. Appl. Phys.*, 51, 2315–2325, 1980.

[45] Kong, J. A., R. Shin, J. C. Shiue, and L. Tsang, "Theory and experiment for passive remote sensing of snowpacks," *J. Geophys. Res.*, 84, 5669–5673, 1979.

[46] Tsang, L. and J. A. Kong, "Microwave remote sensing of a two-layer random medium," *IEEE Trans. Ant. Prop.*, AP-24, 283–287, 1976c.

[47] Zuniga, M. A. and J. A. Kong, "Modified radiative transfer theory for a two-layer random medium," *J. Appl. Phys.*, 51, 5228–5244, 1980.

[48] Zuniga, M. and J. A. Kong, "Mean dyadic Green's function for a two-layer random medium," *Radio Science*, 16, 1255–1270, 1981.

[49] Blinn, J. C., III, J. E. Conel, and J. G. Quade, "Microwave emission from geological materials: Observations of interference effects," *J. Geophys. Res.*, 77, 4366–4378, 1972.

[50] Fung, A. K. and M. F. Chen, "Emission from an inhomogeneous layer with irregular interfaces," *Radio Science*, 16, 289–298, 1981a.

[51] Fung, A. K. and M. F. Chen, "Scattering from a Rayleigh layer with an irregular interface," *Radio Science*, 16, 1337–1347, 1981b.

[52] Fung, A. K. and H. J. Eom, "A theory of wave scattering from an inhomogeneous layer with an irregular interface," *IEEE Trans. Ant. Prop.*, AP-29, 899–910, 1981.

[53] Shin, R. T. and J. A. Kong, "Radiative transfer theory for active remote sensing of homogeneous layer containing spherical scatterers," *J. Appl. Phys.*, 52, 4221–4230, 1981.

[54] Peake, W. H., "Interaction of electromagnetic waves with some natural surfaces," *IEEE Trans. Ant. Prop.*, AP-7, Special Supplement, S324–S329, 1959.

[55] Bass, F. G. and I. M. Fuks, *Wave Scattering from Statistically Rough Surface*, translated by C. B. Vesecky and J. F. Vesecky, Rezamon Press, Oxford, 1979.

[56] Beckmann, P. and A. Spizzichino, *The Scattering of Electromagnetic Waves from Rough Surfaces*, MacMillan, New York, 1963.

[57] Kodis, R. D., "A note on the theory of scattering from an irregular

surface," *IEEE Trans. Ant. Prop.,* **AP-14,** 77–82, 1966.

[58] Lynch, P. J. and R. J. Wagner, "Energy conservation for rough surface scattering," *J. Acoust. Soc. Am.,* **47,** 816–821, 1968.

[59] Lynch, P. L. and R. J. Wagner, "Rough-surface scattering: Shadowing, multiple scatterer and energy conservation," *J. Math. Phys.,* **11,** 3032–3042, 1970.

[60] Sancer, M. I., "Shadow-corrected electromagnetic scattering from a randomly rough surface," *IEEE Trans. Ant. Prop.,* **17,** 577–585, 1969.

[61] Semenov, B., "Approximate computation of scattering electromagnetic waves by rough surface contours," *Radio Eng. Electron. Phys.,* **11,** 1179–1187, 1966.

[62] Stogryn, A., "Electromagnetic scattering from rough finitely conducting surfaces," Radio Science, **2,** 415–428, 1967.

[63] Barrick, D. E., "Relationship between slope probability density function and the physical optics integral in rough surface scattering," *Proc. IEEE,* **56,** 1728–1729, 1968.

[64] Burrows, M. L., "On the composite model for rough surface scattering," *IEEE Trans. Ant. Prop.,* **21,** 241–243, 1973.

[65] Rice, S. O., "Reflection of EM waves by slightly rough surfaces," *The Theory of Electromagnetic Waves,* M. Kline, Ed., Interscience, NY, 1963.

[66] Valenzuela, G. R., "Depolarization of EM waves by slightly rough surfaces," *IEEE Trans. Ant. Prop.,* **AP-15,** 552–557, 1967.

[67] Shen, J. and A. A. Maradudin, "Multiple scattering of waves from random rough surfaces," *Phys. Rev. B,* **22,** 4234–4240, 1980.

[68] Shin, R. T., "Theoretical models for microwave remote sensing of earth terrain," Ph.D. Thesis, MIT, 1984.

[69] Kong, J. A., *Electromagnetic Wave Theory,* Wiley-Interscience, New York, 1986.

[70] Shin, R. T. and J. A. Kong, "Theory for thermal microwave emission from a homogeneous layer with rough surfaces containing spherical scatterers" *J. Geophys. Res.,* **87,** 5566–5576, 1982.